Clim. Past, 19, 419–437, 2023
https://doi.org/10.5194/cp-19-419-2023

Climate of the Past
Open Access
EGU

Sea ice and productivity changes over the last glacial cycle in the Adélie Land region, East Antarctica, based on diatom assemblage variability

Lea Pesjak[1], Andrew McMinn[1], Zanna Chase[1], and Helen Bostock[2,3]

[1]Institute for Marine and Antarctic Studies, University of Tasmania, Hobart, 7000, Australia
[2]School of Earth and Environmental Sciences, University of Queensland, Brisbane, 4072, Australia
[3]National Institute of Water and Atmospheric Research (NIWA), Wellington, New Zealand

Correspondence: Lea Pesjak (lea.pesjak@utas.edu.au)

Received: 29 September 2022 – Discussion started: 4 October 2022
Revised: 23 January 2023 – Accepted: 24 January 2023 – Published: 14 February 2023

Abstract. Although diatoms can provide important palaeoenvironmental information about seasonal sea ice extent productivity, sea surface temperature, and ocean circulation variability, there are still relatively few studies analysing the last glacial cycle near the Antarctic continent. This study examines diatom assemblages over the last glacial cycle from core TAN1302-44, offshore Adélie Land, East Antarctica. Two distinct diatom assemblages were identified using principal component analysis (PC 1–PC 2). The PC 1 assemblage is characterised by *Thalassiosira lentiginosa*, *Actinocyclus actinochilus*, *Eucampia antarctica*, *Azpeitia tabularis* and *Asteromphalus hyalinus* and is associated with the interglacial, sedimentary Facies 1, suggesting that the MIS 5e and Holocene interglacials were characterised by seasonal sea ice environments with similar ocean temperature and circulation. The PC 2 assemblage is characterised by *Fragilariopsis obliquecostata*, *Asteromphalus parvulus* and *Thalassiosira tumida* and is associated with the glacial Facies 2. The variability of PC 2 indicates that, during the MIS 4–2 glacial and the last glaciation, there was an increase in the length of the sea ice season compared with that of the interglacial period, yet there was still no permanent sea ice cover. The initial increase of PC 2 at the start of the glaciation stage and then the gradual increase throughout late MIS 4–2 suggest that sea ice cover steadily increased, reaching a maximum towards the end of MIS 2. The increase in sea ice during glaciation and MIS 4–2 glacial is further supported by the increase in the *Eucampia* index (terminal/intercalary valve ratio), an additional proxy for sea ice, which coincides with increases in PC 2. Aside from the statistical results, the increase in the relative abundance of *Thalassiothrix antarctica* at 40 and 270 cm suggests that, during the last two deglacials, there was a period of enhanced nutrient delivery, which is inferred to reflect an increase in upwelling of Circumpolar Deep Water. Interestingly, the diatom data suggest that, during the last deglacial, the onset of increased Circumpolar Deep Water occurred after the loss of a prolonged sea ice season (decrease in PC 2) but before the ice sheet started to retreat (increase in IRD). Together, these results suggest the changes in sea ice season potentially influenced the ocean's thermohaline circulation and were important factors in driving the climate transitions. The results contribute to our understanding of the sea ice extent and ocean circulation changes proximal to East Antarctica over the last glacial cycle.

1 Introduction

Ocean circulation near Antarctica's ice sheets is changing under the influence of climate change (Pritchard et al., 2009; Depoorter et al., 2013; Alley et al., 2015; Silvano et al., 2018; Rignot et al., 2019; Minowa et al., 2021). The two significant parameters in the atmosphere–ocean–ice sheet interaction system are duration and extent of seasonal sea ice and the ocean's thermohaline circulation. Antarctic sea ice is recognised as an important driver of climate, as it affects the CO_2 exchange between the Southern Ocean and the atmo-

sphere (Crosta et al., 2004; Kohfeld and Chase, 2017), planetary albedo, and the ocean's thermal gradients (Gersonde and Zielinski, 2000). Locally, its seasonal variation can affect ice shelves, increasing melting at the marine edge (Massom et al., 2018), ultimately destabilising the ice sheet (Pritchard et al., 2012). Furthermore, its seasonal expansion and retreat influences primary productivity by limiting light, thus decreasing productivity, although meltwater can also stimulate phytoplankton blooms (Knox, 2006). The second significant parameter affecting climate is the ocean's thermohaline circulation. On the Antarctic margin, this is driven by the formation of Antarctic Bottom Water (AABW) and the upwelling of Circumpolar Deep Water (CDW). Modern observations suggest that Antarctic ice sheet melt rates increase with enhanced upwelling of CDW (Pritchard et al., 2012; Rignot et al., 2019; Minowa et al., 2021), and this causes a decrease in the production of AABW (Williams et al., 2016; Silvano et al., 2018), which may further influence ice sheet melt (Silvano et al., 2018). Understanding the past changes in sea ice and oceanography proximal to Antarctica, especially during past climate transitions and warmer-than-present interglacials, such as the last interglacial, MIS 5e, may provide further insight into the mechanisms of atmosphere–ocean–ice sheet interactions for the prediction of future changes and to provide analogues for future outcomes under a warming climate (Masson-Delmotte et al., 2013).

Studies of diatom assemblages from ocean sediments can be used to reconstruct past ocean environments, including the extent and duration of seasonal sea ice, surface ocean circulation, and productivity (Cooke and Hays, 1982; Pichon et al., 1992; Taylor and McMinn, 2001; Crosta et al., 2004; Gersonde et al., 2005; Armand et al., 2005). Diatom studies are based on the identification and quantification of individual species and groups of species, which are used to reconstruct palaeoenvironments based on an understanding of the species' modern habitat (Table S1 in the Supplement) from both water column (Medlin and Priddle, 1990; Ligowski et al., 1992; Moisan and Fryxell, 1993) and from surface sediment studies (Zielinski and Gersonde, 1997; Armand et al., 2005; Crosta et al., 2005). However, the interpretation can be influenced by processes such as selective dissolution within the water column and/or sediment (Warnock and Scherer, 2015; Shemesh et al., 1989; Zielinski and Gersonde, 1997), winnowing of lighter species' valves by bottom currents (Taylor et al., 1997; Post et al., 2014), or variable influx of terrigenous matter (Kellogg and Truesdale, 1979; Schrader et al., 1993). Therefore, when reconstructing the past environment, it is important to consider all these processes.

There are many diatom-based studies of the interglacials, especially from the Holocene period from the Antarctic continental shelf (McMinn, 2000; Taylor and McMinn, 2001; Leventer et al., 2006; Crosta et al., 2007; Maddison et al., 2012; Peck et al., 2015; Mezgec et al., 2017; Torricella et al., 2021). However, advanced ice sheets, or permanent sea ice, in past glacials led to no diatom productivity over the Antarctic continental shelf and reduced productivity over the slope (Pudsey, 1992; Lucchi et al., 2002; Hartman et al., 2021). Additionally, advancing ice sheets would have removed most of the glacial sediment record from the continental shelves (Domack, 1982; Escutia et al., 2003). This may be one of the reasons why there are so few studies from proximal Antarctica detailing the composition of diatom communities during glacial periods and over the last glacial cycle (Caburlotto et al., 2010; Holder et al., 2020; Hartman et al., 2021; Li et al., 2021; Chadwick et al., 2022).

Overall, limited previous palaeoenvironmental studies based on diatoms from the Antarctic continental slope suggest that, during the last glacial cycle, there was seasonal sea ice cover over the Adélie region (Caburlotto et al., 2010), a permanent sea ice cover in the western Ross Sea (Tolotti et al., 2013), and a prolonged sea ice season in several regions including offshore Cape Adare, the Ross Sea (Hartman et al., 2021), offshore Enderby Land (Li et al., 2021) and offshore the Sabrina Coast (Holder et al., 2020). However, persistent biological productivity has been recorded from offshore Cape Adare (based on diatom studies; Hartman et al., 2021) and the Weddell Sea (based on studies of foraminifera; Smith et al., 2010). These blooms have been suggested to represent localised polynyas (Arrigo and Van Dijken 2003) that existed during the last glacial. Only a couple of studies have looked into climate transitions during the last glacial cycle on the Antarctic margin. They show that, during the last deglacial, there was a decrease of the sea ice season and an increase in upwelling of CDW over the Enderby Land and Ross Sea continental margin (Li et al., 2021; Tolotti et al., 2013), while the last glaciation stage is reported to comprise oscillations in the sea ice season offshore Cape Adare (Hartman et al., 2021). Here we use diatom assemblages to understand the changes in the duration of the sea ice season and in CDW upwelling in the Adélie region over the last glacial cycle, including the glaciation and deglacial transitions.

2 Materials and methods

2.1 Site description

Core TAN1302-44 (Tan_44) was recovered from the WEGA channel on the continental slope north of Adélie Land and the George V Land coastline (Adélie region) at 64°54.75′ S, 144°32.66′ E and from 3095 m depth (Fig. 1) by R/V *Tangaroa* in February 2013 during voyage TAN1302 using a gravity corer with a 2 t head (Williams, 2013). The core site is located ∼ 100 km north off the continental shelf break, within the modern seasonal sea ice zone (Fetterer et al., 2017), covered by sea ice from April to November each year (Fig. 1; Spreen et al., 2008). The major oceanographic features of this region, which directly influence the site (Caburlotto et al., 2006; Williams et al., 2008), include Adélie Antarctic Bottom Water (Adélie AABW), which forms be-

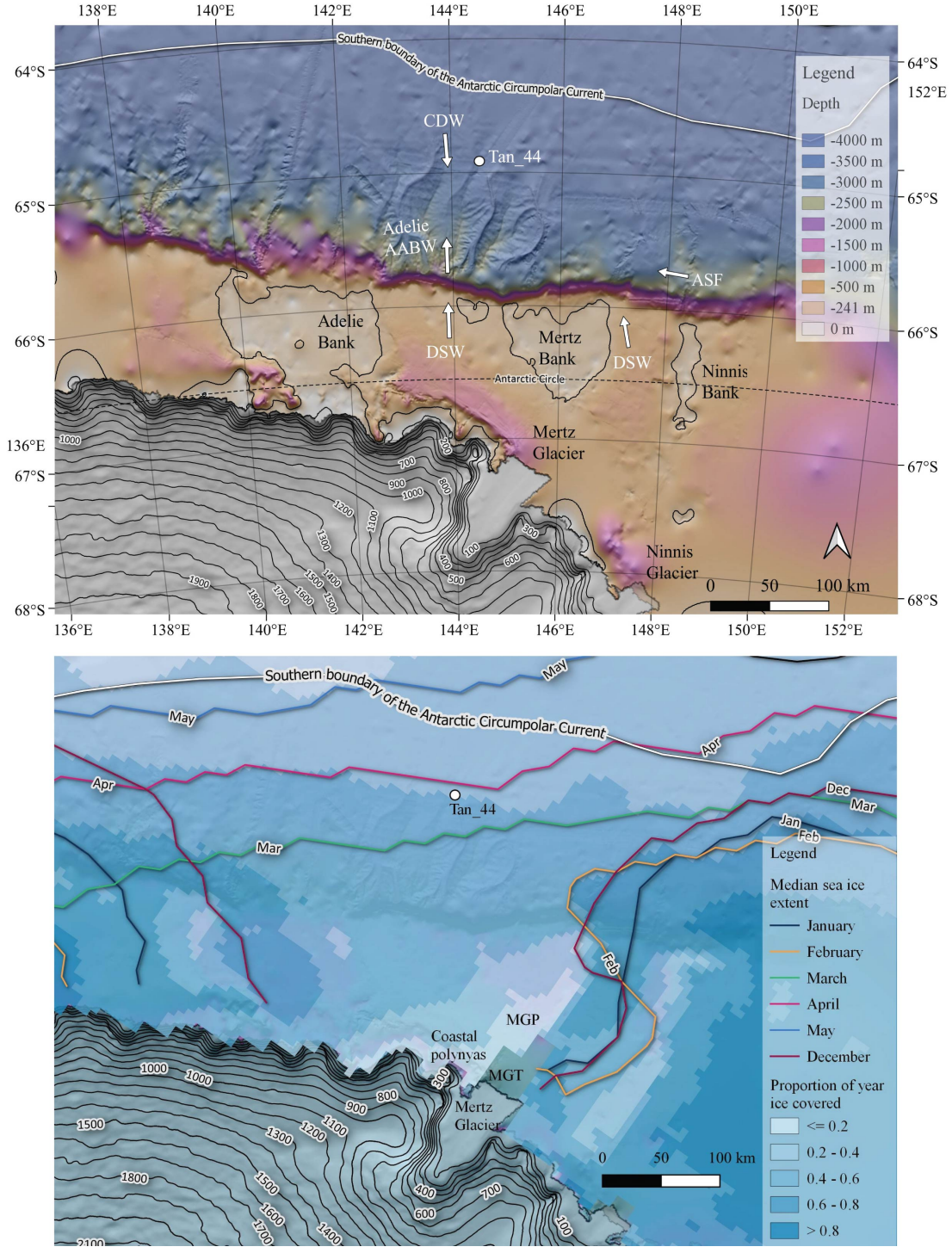

Figure 1. Top panel: location of core Tan_44 with respect to the regional bathymetry (Arndt et al., 2013), oceanography (Orsi et al., 1995; Williams et al., 2010) and cryosphere (Helm et al., 2014). The Mertz and Ninnis glaciers (Helm et al., 2014) are dominant glacial features in the region. Adélie and Mertz banks are prominent geomorphological features on the continental shelf, while deep channels are prominent on the continental slope. Tan_44 is located within the WEGA channel. The site is influenced at present by Adélie-sourced Antarctic Bottom Water (Adelie AABW), Circumpolar Deep Water (CDW) and-along slope flow of Antarctic Slope Front (ASF; Williams et al., 2010). Bottom panel: modern seasonal sea ice cover: the darkest blue shows regions covered by ice for more than 80 % of the year, while the lightest blues indicate areas covered by ice less than 20 % of the year (Spreen et al., 2008), showing the Mertz Glacier polynya (MGP) and the coastal polynyas, where the main proportion of Adélie DSW forms, west of the Mertz Glacier Tongue (MGT; Williams et al., 2010). The figure also shows that the core site is covered by sea ice from April to November each year (coloured lines; Fetterer et al., 2017).

low ∼ 2000 m from the mixing of cooler dense shelf water (DSW), formed on the shelf with warmer and nutrient-rich CDW, and the wind-driven, westward-flowing Antarctic Slope Front ASF (Fig. 1; Jacobs, 1991; Williams et al., 2008). The Antarctic Circumpolar Current (ACC), depicted in Fig. 1 (southern boundary of the Antarctic Circumpolar Current front), does not influence the core site, but the ACC has a significant influence over Southern Ocean productivity and diatom species distribution (Table S1).

2.2 Biogenic silica

Biogenic silica is used in this study as an indicator of paleoproductivity (Bonn et al., 1998; Wilson et al., 2018). Analyses of biogenic silica were undertaken at 20 cm intervals down Tan_44. This study uses a modified wet-leaching technique (Mortlock and Froelich, 1989; DeMaster, 1981), based on the premise that dissolution of fragile-diatom tests is more rapid than the dissolution of silica from non-biogenic sources, e.g., quartz grains. The time series approach introduced by DeMaster (1981) was used. For quality control, two in-house standards were used from the Chilean and Antarctic margins (Tooze et al., 2020). If the silica concentrations of the standards or the samples decreased with time during the hourly measurements, the whole experiment was repeated. The overall reproducibility of the method, assessed as the relative standard deviation of the standards, was ±7 %.

2.3 Si/Al (XRF)

Si/Al is used in this study as an indication of biogenic silica and, therefore, paleoproductivity (Rothwell and Croudace, 2015). X-ray fluorescence scanning (XRF) was completed at 2 mm resolution using an ITRAX scanner (Gadd and Heijnis, 2014) at the Australian Nuclear Science and Technology Organisation (ANSTO). The scanning was performed on u-channel sub-samples of the cores (of dimensions 2 × 2 cm, 1 m long sections), which were stored in plastic containers and covered by thin plastic film. Anomalous spikes in data, identified by eye as significant increases or decreases occurring on mm scale, were removed. The data were then smoothed using a three-point running average.

2.4 Ice-rafted debris (IRD)

Increased ice-rafted debris (IRD) are used in this study as indicators of past Antarctic ice sheet retreat and interglacial periods (Grobe and Mackensen, 1992; Cook et al., 2013; Patterson et al., 2014). IRD analysis was completed using two methods: counting visible grains from X-radiographs (grains ≥ 1 mm, in 5 cm sections) and counting sieved grains (> 500 µm) per dry weight of total sample. The size > 500 µm, medium sand (Patterson et al., 2014) was chosen as the size that defines IRD because laser particle diffraction of samples showed the grain size < 250 µm forms the matrix of all the samples. This is in contrast to other Antarctic studies, which have defined IRD using a range of different sizes from > 2 mm (Grobe and Mackensen, 1992; Diekmann et al., 2004), very coarse sand size, to > 1 mm (Lucchi et al., 2002; Pudsey and Camerlenghi, 1998), > 250 µm (Wilson et al., 2018) and > 125 µm (Cook et al., 2013; Passchier, 2011).

2.5 Facies and age model

Radiocarbon dating was undertaken to support age model development using the acid-insoluble organic matter (AIOM) method, conducted at ANSTO, Sydney, in April 2017 according to Hua et al. (2001), Fink et al. (2004) and Stuvier and Polach (1977). The raw radiocarbon ages were calibrated using CALIB, version 7.1; Marine13 calibration curve (Reimer et al., 2013); and the regional variation to the global marine reservoir correction, ΔR, of 830 yr ± 200 yr, following previous work done in this region by Domack et al. (1989).

A facies model was developed using the lithological unit characteristics (Sect. S1.2.1 in the Supplement) and the combination of other data, primarily biogenic silica, Si/Al and ice-rafted debris (IRD). The definition of facies was designed to capture large variability in the physical and geochemical quality of sediment, including large changes in productivity (biogenic silica, Si/Al and Ba/Ti) and sedimentology (IRD content; Wilson et al., 2018; Salabarnada et al., 2018; Wu et al., 2017; Bonn et al., 1998; Grobe and Mackensen, 1992; Patterson et al., 2014).

The age model of Tan_44 is based on the facies model and two radiocarbon dates from the top 25 cm of the core, using the premises that variability in facies, including large changes in productivity proxies (biogenic silica, Si/Al and Ba/Ti) and IRD content, present glacial to interglacial climate variability (Wilson et al., 2018; Salabarnada et al., 2018; Wu et al., 2017; Bonn et al., 1998; Grobe and Mackensen, 1992; Patterson et al., 2014).

2.6 Diatom counts and Shannon–Wiener biodiversity index

Diatom species were counted from samples taken every 10 cm down core Tan_44 (starting at 5 cm, then 20 cm). The samples were processed following the methods outlined in Taylor and McMinn (2001). A small section of the sediment core (< 0.5 cm thick) was soaked in 15 % hydrogen peroxide overnight to remove organic matter and to disaggregate any clay. The samples were rinsed with deionised water through a 100 and a 10 µm sieve in order to obtain a > 10 but < 100 µm grain fraction. This fraction was left overnight to settle. Excess water above the sample was pipetted out, and the remaining sample was stored in a 100 mL tube. A drop from each shaken tube was pipetted onto a glass cover slip over a hotplate at 50 °C to evaporate excess water. The samples were then mounted with Norland Optical Adhesive 61 and

cured in sunlight. Diatom identification and counts were undertaken using a Nikon light microscope (Eclipse Ci, DS-Ri2) at 1000 x magnification. Each sample was traversed until > 400 valves were counted. Broken valves that were > 50 % complete were included in the count, and in the case of elongated species, such as *Thalassiothrix* and *Trichotoxon*, that are subject to fragmentation, only the ends were counted (McMinn et al., 2001). Lower valve numbers of less than 400 valves per slide were encountered in samples at 80 cm and from 350–300 cm. The numbers of valves within the 350–320 cm samples were extremely low (7–16 valves per slide). Due to the scarcity of valves in these samples (well below 400 valves per slide were observed within 320–300 cm), only samples from 290–5 cm are included in statistical analysis.

Some species were grouped together due to morphology and habitat indicators; these groups are the *Fragilariopsis* group, comprising *F. obliquecostata*, *F. sublinearis*, *F. linearis*, and *F. cylindrus*; the *Thalassiothrix* group, comprising *Thalassiothrix antarctica*, *Thalassiothrix longissima* and *Trichotoxon reinboldii*; and the *Rhizosolenia* group, comprising *Rhizosolenia antennata* var. *semispina*, *Rhizosolenia antennata* var. *antennata*, *R. simplex*, *R. polydactyla var polydactyla*, *Rhizosolenia* sp. and *Proboscia inermis*.

The relative abundance of each species (or group) was expressed as the number of valves of that species divided by the total valve count (expressed as %). Species or species groups with > 1.8 % in at least two samples were included in statistical analysis, except in the case of the *Fragilariopsis* group, which, apart from *Fragilariopsis obliquecostata* (present at > 1.8 % in at least two samples), also included the much rarer sea ice species *F. sublinearis*, *F. linearis* and *F. cylindrus*.

Species or species groups present at > 1.8 % in at least one sample, and thus excluded from statistics, were included in results and discussion due to their environmental indications (Table S1). These species include the *Thalassiothrix antarctica* group, represented mainly by *Thalassiothrix antarctica*, and the *Rhizosolenia* species group, represented mainly by *Rhizosolenia antennata* var. *semispina* and *Rhizosolenia antennata* var. *antennata* (the sum of both species was up to 1.2 %–1.6 % in three samples). The *Thalassiothrix* group is also discussed where there is a significant increase in broken valves but the relative abundance (i.e., counted valve ends) is 0 %.

The *Eucampia* index was used as an indicator of sea ice presence (Fryxell, 1991). It represents the ratio of the number of terminal valves to the number of intercalary valves of *Eucampia antarctica* species, and its increase is associated with more sea ice in the environment. In the open ocean, the *Eucampia antarctica* species grow in longer chains, while in sea ice waters they grow in shorter chains (Fryxell, 1991). The chains comprise intercalary valves in the middle and terminal valves at the ends – therefore, the more terminal valves, the more sea ice (Fryxell, 1991: Kaczmarska et al., 1993). The *Eucampia* index was only calculated where the total *Eucampia antarctica* count was 100 valves and above.

An assessment of the diversity of diatoms in each sample was determined using the Shannon–Wiener diversity index. The Shannon–Wiener diversity index (Spellerberg and Fedor, 2003) was calculated according to the following formula:

$$H = -\sum_{i=1}^{n} \left[p_i x \ln p_i \right]. \quad (1)$$

2.7 Statistical analyses: cluster analysis and principal component analysis

The relative diatom abundance data set was analysed using a hierarchical cluster analysis and principal component analysis (PCA) in the Statistical Package for Social Sciences (SPSS) software package. For these analyses, the relative abundance data were logarithmically transformed using the following equation: Abundance $= \log_{10}(x + 1)$, where $x =$ relative abundance (%) (Taylor et al., 1997). Cluster analysis (Burckle, 1984; Truesdale and Kellogg, 1979) involved calculating the average distance between groups. The PCA (Taylor et al., 1997; Zielinski and Gersonde, 1997) was undertaken in two stages. In Q mode, investigating relationships between variables (species), and in R mode, analysing relationships between samples (Shi, 1993). The factor variance used to extract the number of components for Q mode analysis was established at ≥ 12 % variance. The factor variance used to extract the number of components for R mode analysis was established at ≥ 42 %. Factor variance is the amount of the total variance of all of the variables accounted for by each component (factor) (https://www.ibm.com/docs/en/spss-statistics, last access: 20 July 2020; https://www.ibm.com/docs/en/spss-statistics, last access: 20 July 2020; IBM, 2020). Outputs from both Q and R analyses underwent a varimax rotation. Rotation maintains the cumulative percentage of variation explained by the chosen components, but the variation is spread more evenly over the components (https://www.ibm.com/docs/en/spss-statistics, last access: 20 July 2020; IBM, 2020). Finally, to demonstrate the strength of the correlation between the components and productivity proxies (Si/Al and biogenic silica), bivariate Pearson correlation analyses were undertaken using SPSS.

3 Results

3.1 Biogenic silica, Si/Al, ice-rafted debris and the facies model

The facies model is comprised of four facies which alternate down core (Fig. S1 in the Supplement; Table 1). The main parameters determining the facies (biogenic silica, Si/Al and IRD) are described below. The interpretation of the facies is further described in the "age model" section.

Table 1. Summary of the characteristics of the four facies present in core Tan_44.

Characteristics	Facies			
	1 Olive sandy mud	1A Olive mud	2 Grey mud	2A Olive grey mud
Structure	Massive; bioturbation; rare laminae	Massive; bioturbation	Massive; bioturbation; laminae; traction structures	Massive; bioturbation
Colour	Olive; grey (base layer)	Olive	Grey	Olive grey
IRD (grains per 5 cm)	2–36	0–10	0–14	1–15
IRD (grains per gram)	2–15	0–1	0–1	0–2
% Vf-f sand	1–19	1–7	0–5	0–6
% Vc silt	8–27	3–18	4–13	7—7
Zr/Rb	0.6–2.3	0.5–1.9	0.4–1.4	0.7–1.4
% biogenic silica	3–22	4–10	3–18	10–11
Si/Al	15–28	14–23	12–20	16–21
Ba/Ti	0.01–0.06	0–0.06	0–0.04	0.03–0.05
Interpretation	Interglacial	Deglacial	Glacial	Glaciation

Table 2. Radiocarbon dating (AIOM) conventional and calibrated results.

Lab no.	Sample	Depth (cm)	Conventional radiocarbon age (yr BP)	Error ± yr	$\delta^{13}C$	Calibrated age (cal yr BP); $\Delta R = 830 \pm 200$ yr	Calibrated mean (yr BP)
OZV390	Tan44_0cm	0.5–3.5	5765	45	−25	4971–5478	5233
OZV391	Tan44_25cm	25.5–26.5	14 660	80	−23.6	15 837–16 468	16 160
OZV392	Tan44_35cm	35.5–36.5	18 470	90	−23.9	20 504–21 082	20 803
OZV393	Tan44_45cm	45.0–46.0	19 150	140	−25	21 340–22 007	21 682

Biogenic silica varied from 0 %–22 % (Figs. S1, 2 and 3; Table 1). The highest values were found in the top 40 cm (10 %–22 %), at 260–140 cm (12 %–16 %) and at the base of the core at 540–520 cm (3 %–11 %), coinciding with olive and grey sandy mud (Facies 1) and olive grey mud (Facies 1A). Moderate to low values (3 %–10 %) occurred in olive mud (Facies 2A) and grey mud (Facies 2), with the exception of 18 % at 140 cm within Facies 2 (Figs. S1 and 3).

Si/Al (XRF) values varied from 14–28 (Figs. S1, S2, 2 and 3; Table 1). Higher values occurred within olive and grey sandy mud (Facies 1), while lower values occurred within olive mud (Facies 2A), olive grey mud (Facies 1A) and grey mud (Facies 2).

High counts of ice-rafted debris (IRD; 2–36 grains per 5 cm) are found in olive and grey sandy mud (Facies 1; Figs. S1, 2 and 3; Table 1), with maximum counts found at 15–10, 255–250 and 500–495 cm. Lower numbers of IRD (0–14 grains per 5 cm) are found in grey mud (Facies 2), olive grey mud (Facies 1A) and olive mud (Facies 2A).

3.2 Radiocarbon dates and the age model

The two top radiocarbon dates (Fig. 2) indicate that the top of the core was deposited between 16.2–5.2 ka, suggesting Facies 1 is of Holocene and Facies 2A of Late Pleistocene age. Facies 1 at 270–230 cm is interpreted as being the last interglacial MIS 5e, supported by the fact that we did not observe any *Rouxia leventerae* (last occurrence at MIS 6–5e boundary; Zielinski and Gersonde, 2002) at these depths. The two deeper radiocarbon dates (Table 2) were not included in the interpretation because they imply an unreasonably high sedimentation rate. Similar unreasonable C-14 dates at similar core depths, and even age reversals, were observed in other cores from the region (Pesjak, 2022).

The main characteristics of the facies found in Tan_44 (Table 1), in combination with the radiocarbon dates at the top of core, suggest that glacial to interglacial variability influenced the productivity proxies (biogenic silica, Si/Al and Ba/Ti; Wilson et al., 2018; Salabarnada et al., 2018; Wu et al., 2017; Bonn et al., 1998; Grobe and Mackensen, 1992) and IRD (Patterson et al., 2014; Figs. S1 and 2), which show a strong

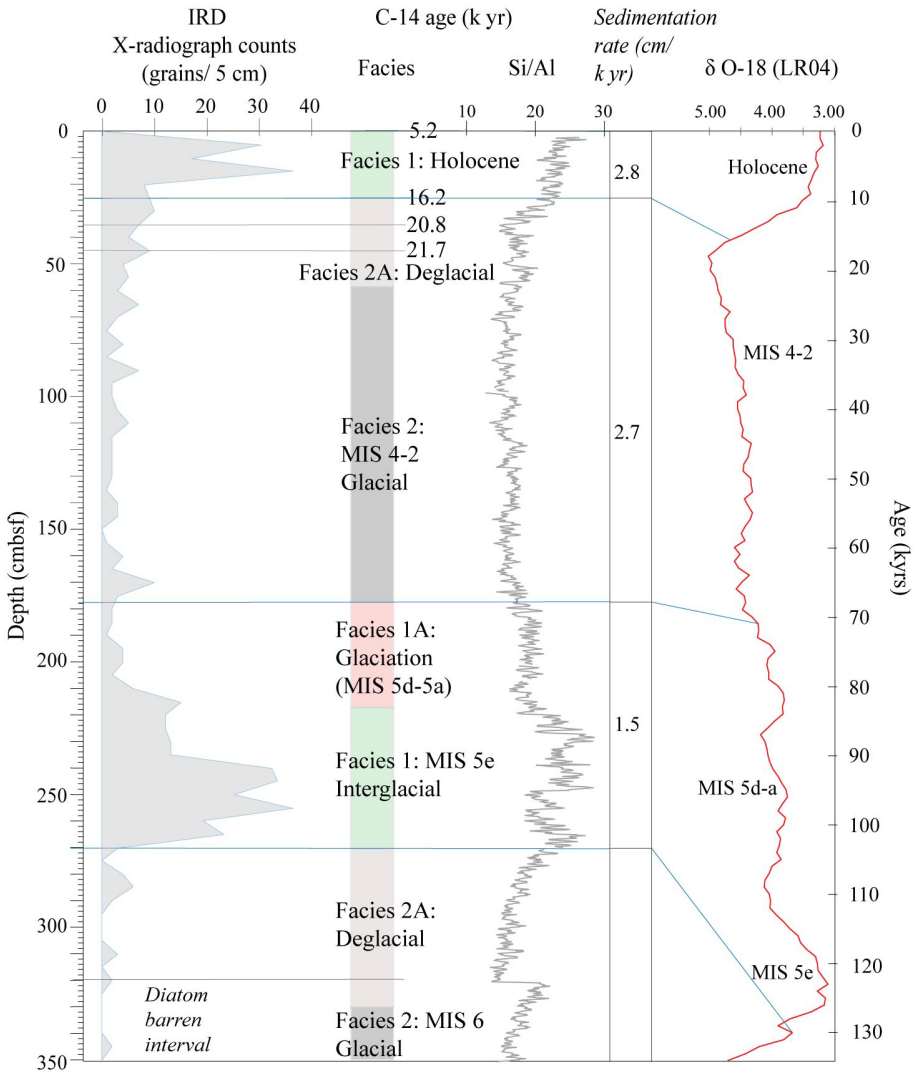

Figure 2. IRD counts, facies model and Si/Al for core Tan_44. The age model is based on the facies model and is supported by radiocarbon dating of two depths at the top of the core and the comparison of Si/Al to the global benthic stable isotope stack LR04 (Lisiecki and Raymo, 2005).

coincidence with the global benthic $\delta^{18}O$ stack (Lisiecki and Raymo, 2005).

3.3 Species distribution, biodiversity and abundance

All samples contained well-preserved diatom assemblages with little evidence of dissolution, such as frustule thinning. Of the 52 species identified in 34 samples (Table S4), 24 species (Table S1) were included in the species distribution description, and of those, 15 species were included in statistical analysis (12 species with an additional 3 included as part of the *Fragilariopsis* group; Fig. 3). One extinct species, *Actinocyclus ingens* (Cody et al., 2008), was found at 11 % at 60 cm and at 3 % at 280 cm, both at the glacial-to-deglacial facies boundaries MIS 2–1 and MIS 6–5e. Shannon–Wiener index values were relatively high (1.6–2) at 40 cm and at 220–130 cm within the glaciation and glacial (MIS 4–2) facies (Fig. 3). The interval from 350–320 cm is considered barren (Fig. 3); it contains only a few specimens of robust valve forms such as *Thalassiosira lentiginosa*, *Eucampia antarctica* and *Actinocyclus actinochilus* (Table S4). This interval also contains pyritised shells, which were also found at 80–60 cm during the Last Glacial Maximum (Fig. S1). The distribution of species (between 290–5 cm depth) is described below, in the order of species habitats (Table S1).

The most abundant species in the samples were those associated with open ocean environments: *Thalassiosira lentiginosa* (20 %–73 % of the total counts), *Eucampia antarctica* (2 %–62 %) and *Fragilariopsis kerguelensis* (1 %–25 %;

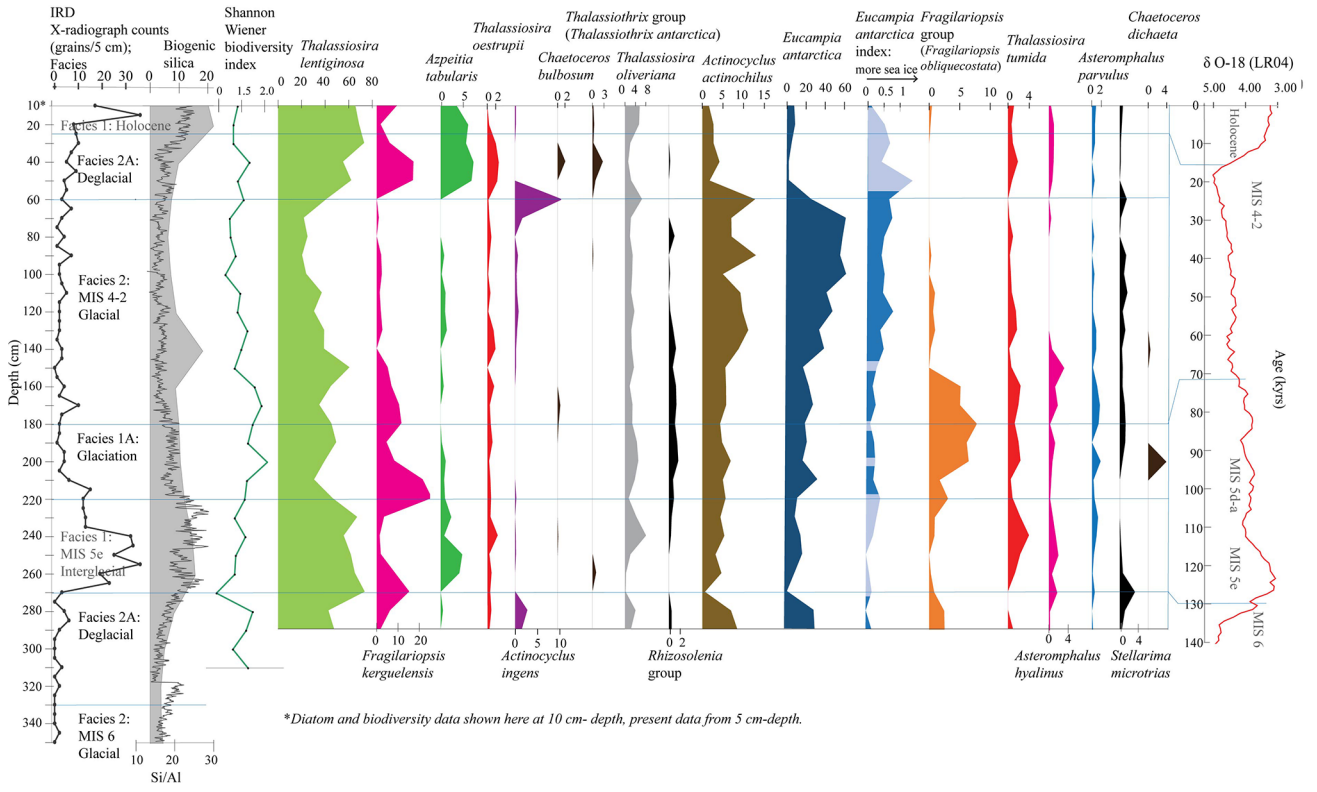

Figure 3. Tan_44 distribution of main species, species groups and *Eucampia* index (terminal/intercalary valve ratio). Results include IRD counts, facies interpretation (vertical lines), biogenic silica (%), Si/Al (XRF) and the Shannon–Wiener biodiversity index. The facies model is shown in comparison to LR04 (Lisiecki and Raymo, 2005). Species in black are not included in statistical analysis due to lower abundance (> 1.8 % in just one sample). These are the *Rhizosolenia* group (mainly *Rhizosolenia antennata* var. *semispina* and *Rhizosolenia antennata* var. *antennata*), the *Thalassiothrix* group (mainly *Thalassiothrix antarctica*), *Stellarima microtrias*, *Chaetoceros bulbosum* and *Chaetoceros dichaeta*. *Eucampia* index was also not included in statistical analysis; its distribution in dark blue shows where total *Eucampia antarctica* counts are > 100 valves per sample, while the light blue areas show samples with < 100 counts.

Fig. 3). The highest abundance of *Thalassiosira lentiginosa* (> 55 %) occurred at 50–5 cm (interglacial and deglacial facies), at 150 cm (glaciation) and at 270–230 cm (interglacial). The highest abundance of *Eucampia antarctica* (18 %–62 %) occurred at 210–60 cm (glacial and glaciation), at 290–280 cm (deglacial) and at 250 cm (interglacial). Maximum *Fragilariopsis kerguelensis* (17 %–25 %) was found at 220–210 cm (glaciation) and at 50–40 cm (deglacial). Less abundant open ocean species (Fig. 3) included *Thalassiosira oliveriana* (highest abundance of 4 %–8 %) at 20–5, 60, 200–190, 240–230 and 280 cm, within interglacial, deglacial and glacial facies; *Azpeitia tabularis*, with an abundance of 3 %–6 % at 50–5 and 260–250 cm, within the interglacial and deglacial facies; *Chaetoceros bulbosum*, with 4 %, at 40 cm, within the deglacial facies; *Chaetoceros dichaeta*, with 4 %, at 200 cm, within the glaciation facies; *Asteromphalus hyalinus*, with 2 %–3 %, at 150, and 250 cm, within the glacial facies. The *Thalassiothrix* group, dominated by *Thalassiothrix antarctica*, had a relative abundance of 3 % at 40 cm (Fig. 3) and a high amount of broken valves relative to other samples at 40, and 270 cm (Fig. 5), although the 270 cm sample had 0 % relative abundance (i.e., valve ends counted). Both intervals occur within the deglacial facies. *Thalassiosira oestrupii* had an abundance of 2 %–3 % at 50–30 cm (deglacial) and 240 cm (interglacial); *Asteromphalus parvulus* had an abundance of 1.8 % at 170 cm and 2 %, at 200 cm, within the glacial facies; and the *Rhizosolenia* group, dominated by *Rhizosolenia antennata* var. *semispina* and less by *Rhizosolenia* antennata var. *antennata*, had a relative abundance of 1.8 %–1.9 % at 140, 170 and 200 cm, within the glacial facies.

Open ocean sea ice edge species (Table S1) were comprised of *Actinocyclus actinochilus*, which showed a 7 %–13 % abundance at 140–50 and 290–280 cm, within glacial and deglacial facies, and *Thalassiosira tumida*, which showed a 2 %–4 % abundance at 170–160 and 200–190 cm, within the glacial facies, and at 250–230 cm, within the interglacial facies.

Sea ice proxies (Table S1) were comprised of the *Fragilariopsis* group species, *Eucampia* index and *Stellarima microtrias*. The *Fragilariopsis* group was comprised of the dominant species *Fragilariopsis obliquecostata* and much lower abundances of *F. sublinearis*, *F. linearis* and *F. cylindrus*.

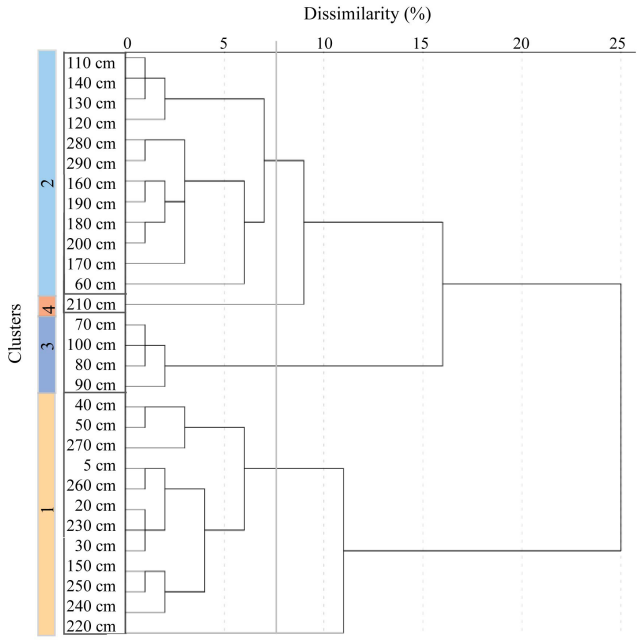

Figure 4. Hierarchical cluster analysis dendrogram illustrating agglomeration of four clusters at dissimilarity of 7 %.

Fragilariopsis obliquecostata is a species that lives in sea ice (Crosta et al., 2022; Garrison and Buck, 1989; Armand et al., 2005). The *Fragilariopsis* group attained maximum abundances from 5 %–8 % at 160–200 cm, within the glacial facies. The *Eucampia* index is elevated between 140–60 cm within the late MIS 4–2 glacial facies. The *Eucampia* index is not considered at intervals within 50–5, and 270–220 cm and at depths of 150, 180 and 200 cm (Fig. 3) due to *Eucampia antarctica* counts being < 100 valves per sample, which is considered too low to be statistically reliable. *Stellarima microtrias* was found to be > 2 % only at 270 cm, within the deglacial facies.

3.4 Cluster and principal component analyses

Cluster analysis groups are sampled according to the similarity of the sample assemblages (Shi, 1993). The groupings, illustrated by a dendrogram, can represent similar environments and therefore aid in the reconstructions of palaeoenvironments. Based on the relative abundance of diatom species, four clusters were identified (Fig. 4), with a dissimilarity index of 7 %. The two largest groups, Cluster 1 and Cluster 2, correlate well with the interglacial and glacial facies, respectively (Fig. 4).

Cluster 1 includes samples from 5–50, 150 and 270–220 cm. This cluster, which contains open ocean species (Fig. 3), is associated with mainly the interglacial, deglacial and, much less, glacial facies. Cluster 2 includes samples from 140–110, 200–160 and 60 cm. This cluster is mainly associated with the glacial facies, represented by sea ice and ice edge species (Fig. 3). Cluster 3 includes samples from 100–70 cm and is associated with the glacial facies. Cluster 4 is represented by only one sample, at 210 cm, within the glaciation facies.

The Q mode PCA analysis identified three components that together explained 54 % of sample variance (Tables S2 and 3). Component 1 (PC 1) explains 26 % of the variance and contains contributor species associated with open ocean and sea ice edge environments. Species determining this component are *Thalassiosira lentiginosa*, *Actinocyclus actinochilus*, *Eucampia antarctica*, *Azpeitia tabularis* and *Asteromphalus hyalinus*. Component 2 (PC 2) explains 16 % of the variance and is associated with sea ice or the coastal Antarctic environment. These are the *Fragilariopsis* group (dominated by *Fragilariopsis obliquecostata*), *Asteromphalus parvulus* and *Thalassiosira tumida*). Component 3 (PC 3) explains 12 % of the variance, and its contributor species are associated with an open ocean environment. These are *Actinocyclus ingens*, *Actinocyclus actinochilus* and *Thalassiosira oliveriana*.

The R mode PCA analysis identified three components, explaining 99 % of the down-core variance (Table S3; Fig. 5). The variance is mostly explained by PC 1 and PC 2. PC 1, the open ocean assemblage, explains 54 % of the variance and shows high factor loadings at 40–5 and 270–150 cm. Both of these intervals coincide with Clusters 1, 2 and 4, within the interglacial, deglacial, glaciation and early MIS 4–2 glacial facies. PC 2, the sea ice and ice edge species assemblage (Table 3), explains 42 % of the variance and shows high factor loadings at 140–70, 170, 210 and 290–280 cm. These intervals coincide with Clusters 2 and 3, within the glacial facies, and Cluster 4, within the glaciation facies (Fig. 5).

3.5 Correlation between diatom assemblages and productivity

Correlation analysis shows a strong statistical relationship between PC 1 and PC 2 assemblages and Si/Al and biogenic silica (Table 4). PC 1 assemblage shows a positive correlation to Si/Al ($r = 0.63$) and to biogenic silica ($r = 0.57$). PC 2 shows a negative correlation to Si/Al ($r = -0.62$) and to biogenic silica ($r = -0.54$). All correlations are statistically significant ($p < 0.001$).

4 Discussion

4.1 Diatom assemblages, clusters and sedimentary facies

Principal component analysis distinguished three diatom assemblages. PC 1 and PC 2 assemblages incorporated most of the variance (42 %–54 %), while PC 3 was much less influential (accounting for ~ 2 % of total variance; Fig. 5). The assemblages and their environmental interpretation are described below. Due to PC 3 contributing a minor amount

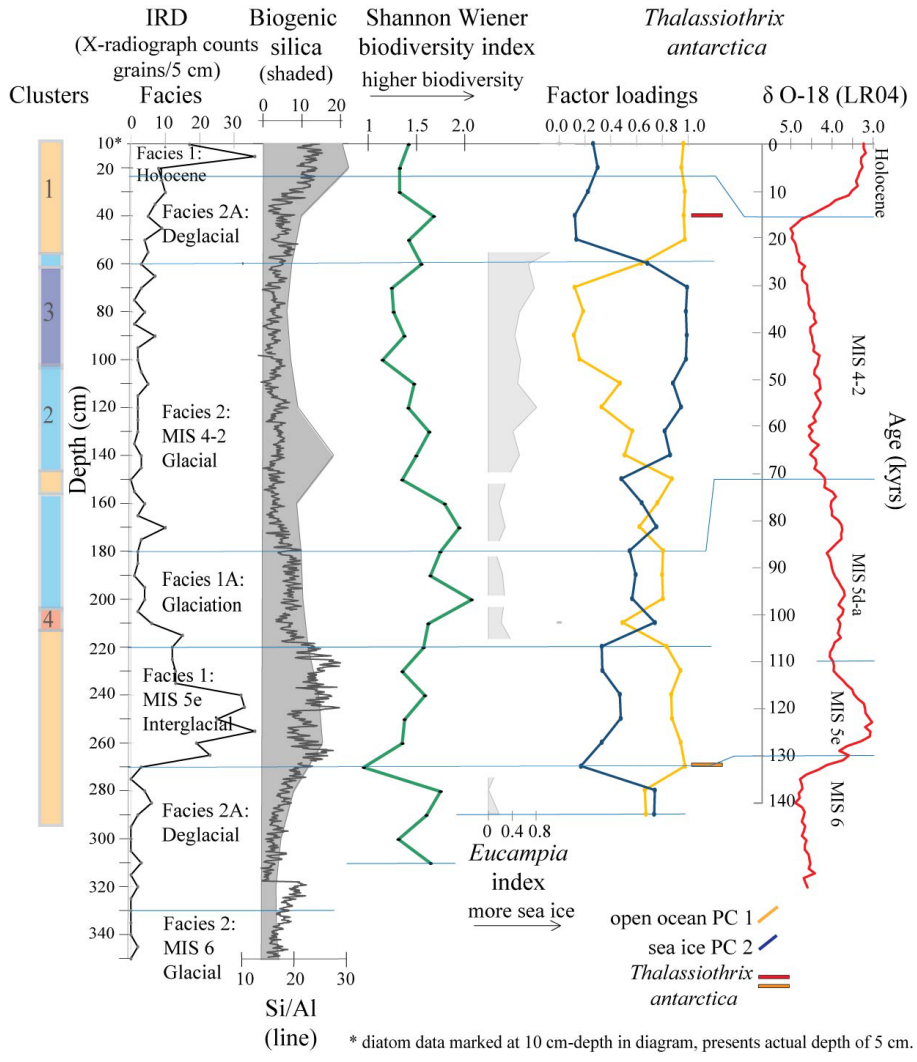

Figure 5. Principal component PC 1 and PC 2 factor loadings down core Tan_44, *Eucampia* index, *Thalassiothrix antarctica*, and Shannon–Wiener biodiversity index (green). Also included are cluster results, IRD counts, sediment facies (horizontal lines), biogenic silica, Si/Al and LR04 curve (Lisiecki and Raymo, 2005). *Eucampia* index results are presented here only at depths where total *Eucampia antarctica* counts > 100 valves per sample. *Thalassiothrix antarctica* (red and orange) show depths with abundant broken valves, where the 270 cm sample (orange) comprised 0 % relative abundance of counted valve ends.

of variance to the samples, it is defined here, but it is not used in the environmental interpretations. Separately from the statistics, the *Eucampia* index and the presence of lower abundances of indicator species (particularly the *Thalassiothrix* group), which indicates high productivity, are further discussed.

4.1.1 The open ocean assemblage (PC 1)

The PC 1 assemblage comprises the open ocean species *Thalassiosira lentiginosa*, *Eucampia antarctica* and *Asteromphalus hyalinus* (Johansen and Fryxell, 1985; Garrison and Buck, 1989; Medlin and Priddle, 1990; Zielinski and Gersonde, 1997); the ice edge species *Actinocyclus actinochilus* (Medlin and Priddle, 1990; Ligowski et al., 1992; Garrison and Buck, 1989; Armand et al., 2005); and the warmer-water species *Azpeitia tabularis* (Zielinski and Gersonde, 1997; Romero et al., 2005). Therefore, the PC 1 assemblage is interpreted to represent an open ocean environment: a relatively warmer ocean with seasonal sea ice cover (Table 3) and high productivity, similar to the modern-day environment over the core site.

The composition of the PC 1 assemblage further suggests that selective species preservation, due to reworking by bottom currents and/or dissolution processes, had been active. The presence of a combination of robust species, e.g., *Eucampia antarctica* and *Actinocyclus actinochilus*, suggests that some level of reworking of sediments (Shemesh

Table 3. Species assemblages (PC 1–PC 3) according to Q mode principal component analysis (further information can be found in Table S2).

Factor loadings	Assemblage	Environment
P 1		
$> 0.5/ > -0.5$	*Thalassiosira lentiginosa*	Open ocean
	Eucampia antarctica	
	Azpeitia tabularis	
	Asteromphalus hyalinus	
	Actinocyclus actinochilus	Sea ice edge
P 2		
> 0.5	*Fragilariopsis* group*	Sea ice
	Thalassiosira tumida	Ice edge
	Asteromphalus parvulus	Coastal
P 3		
> 0.5	*Actinocyclus ingens*	Reworked
	Actinocyclus actinochilus	
	Thalassiosira oliveriana	

* Mainly *Fragilariopsis.obliquecostata*.

Table 4. Correlation (r) between each PC component and Si/Al and biogenic silica.

	r value	
Assemblage	Si/Al	Biogenic silica
PC 1 open ocean	0.63*	0.57*
PC 2 sea ice	−0.62*	−0.54*

* Statistically significant correlation ($p < 0.001$).

et al., 1989; Taylor et al., 1997) or dissolution (Warnock and Scherer, 2015) influenced the assemblage composition. These species have been found within assemblages considered to have been influenced by reworking offshore Cape Darnley in Prydz Bay (Taylor et al., 1997) and the continental slope of the Ross Sea (Truesdale and Kellogg, 1979). Reworking is corroborated by the knowledge that the site is currently influenced by the down-slope flow of Adélie AABW and along-slope currents, including the ASF (Fig. 1; Williams et al., 2008). Furthermore, the presence of unusual abundances of *Thalassiosira lentiginosa* (Fig. 3), a species usually associated with open ocean assemblages (Taylor et al., 1997; Truesdale and Kellogg 1979; Crosta et al., 2005) and that has been associated with dissolution (Shemesh et al., 1989), further supports that some level of dissolution had affected the PC 1 assemblage composition. Such high abundances of *T. lentiginosa* are not observed in modern sediments in the Adélie region (Leventer, 1992) or elsewhere within the sea ice zone on the Antarctic margin (Zielinski and Gersonde, 1997; Armand et al., 2005; Crosta et al., 2005). Despite the influence of reworking and dissolution, the PC 1 assemblage is still considered to be primarily autochthonous and dominated by in situ deposition associated with open ocean, warmer-water, and sea ice edge species. The presence of *Azpeitia tabularis* and *Asteromphalus hyalinus*, species not commonly associated with reworking or dissolution, further confirms this position.

4.1.2 The sea ice assemblage (PC 2)

The largest contributions to the PC 2 assemblage (Table 3) are from the *Fragilariopsis* group, comprising mainly *Fragilariopsis obliquecostata*, a species which currently lives in sea ice and at the sea ice edge (Ligowski et al., 1992; Medlin and Priddle, 1990; Moisan and Fryxell, 1993). In the Antarctic continental margin surface sediments from the Ross Sea, Weddell Sea and Prydz Bay, *Fragilariopsis obliquecostata* appears where sea ice cover is present > 7 months per year (Armand et al., 2005). Other species in PC 2 include the coastal species *Asteromphalus parvulus* (Kopczyńska et al., 1986; Scott and Thomas, 2005) and the open water and sea ice edge species *Thalassiosira tumida* (Garrison and Buck, 1989). Based on a combination of sea ice, sea ice edge and coastal species, the PC 2 assemblage is interpreted as resulting from an environment proximal to the permanent sea ice edge, with a long sea ice duration of > 7 months, as currently observed in the Ross and Weddell seas (Fetterer et al., 2017).

4.1.3 The reworked assemblage (PC 3)

The PC 3 assemblage comprises *Actinocyclus ingens*, *Actinocyclus actinochilus* and *Thalassiosira oliveriana* (Table 3). *Actinocyclus ingens* is an extinct species, with last appearance datum (LAD) 0.43–0.5 Ma (Cody et al., 2008). *Thalassiosira oliveriana* is a species associated with open ocean environments (Medlin and Priddle, 1990), while *Actinocyclus actinochilus* is associated with sea ice edge environments (Medlin and Priddle, 1990; Garrison and Buck, 1989). However, these species (including *A. ingens*) have robust valves that can survive transport by bottom currents (Shemesh et al., 1989; Taylor et al., 1997; Truesdale and Kellogg, 1979). PC 3 is therefore interpreted as a reworked assemblage (allochthonous), transported from elsewhere by bottom water transport, with no in situ deposition and hence no environmental signal. The reworking is supported by the presence of extinct *Actinocyclus ingens*, which is only found at 60 and 290–280 cm depth (Fig. 3). The 60 cm interval also contains pyritised shells (Fig. S1). Due to its very small influence on variability, the PC 3 assemblage is not considered further in the palaeoenvironmental interpretation of Tan_44.

4.1.4 *Thalassiothrixantarctica* – a high-productivity proxy

Aside from statistical analysis, the down-core distribution of the *Thalassiothrix* group, of which *Thalassiothrix antarctica* is the most common species, is considered to be an environmental indicator (Figs. 3 and 5). *Thalassiothrix antarctica*, as well as the other two species which make up this group, *Thalassiosira lentiginosa* and *Trichotoxon reinboldii*, are open ocean species (Kopczyńska et al., 1998; Garrison and Buck, 1989; Beans et al., 2008). *Thalassiothrix antarctica* and *Thalassiothrix longissima* are found in surface sediments, between coastal Antarctica and the subtropical front (Zielinski and Gersonde, 1997). While *Trixotoxon reinboldii* is associated with sediment from colder or ice edge waters (Crosta et al., 2005), *Thalassiothrix antarctica* is also associated with diatom blooms that occur in modern coastal and shelf waters, such as in Prydz Bay (Ligowski, 1983; Quilty et al., 1985), or in naturally fertilised areas, such as the Kerguelen Plateau (Rembauville et al., 2015). Zielinski and Gersonde (1997) consider *Thalassiothrix antarctica* from the Weddell Sea sediments to be indicators of high productivity. *Thalassiothrix antarctica* is not found in modern sediments off the Adélie region (Leventer, 1992). However, Beans et al. (2008) found that this species can sometimes be abundant in waters offshore Adélie Land. Based on the conclusions of Zielinski and Gersonde (1997) and Rembauville et al. (2015), the abundance of the *Thalassiothrix* group, represented largely by *Thalassiothrix antarctica* species, is indicative of a higher-nutrient environment and higher productivity than in the present Adélie region, which we associate with increased upwelling of the Circumpolar Deep Water.

4.2 Palaeoecological interpretation

4.2.1 Interglacial (MIS 5e and Holocene)

The interglacial facies is associated with PC 1 (open ocean assemblage; Fig. 5; Table 3) and, to a lesser extent, with PC 2 (sea ice assemblage). The dominance of the PC 1 assemblage suggests that the Holocene and MIS 5e environments had seasonal sea ice, with open ocean during the summer and sea ice cover during winter, spring and autumn, similar to the modern situation (Fig. 1). The inference of the seasonal presence of sea ice is strengthened with the moderate presence of the PC 2 assemblage, which represents increased sea ice duration. PC 1 also provides evidence of a reworked and dissolution-affected assemblage. Indeed, strong bottom currents, such as AABW and ASF, which sweep the continental slope offshore Adélie Land at present (Fig. 1; Williams et al., 2010), may have been active throughout the Holocene and MIS 5e. Furthermore, the reworking by bottom currents may have been stronger at times. Lastly, the PC 1 assemblage is associated with elevated productivity, which is supported by high Si/Al and biogenic silica but lower biodiversity (Fig. 5). Low biodiversity is likely affected by poor preservation (dissolution and reworking) but potentially also reflects modern diatom blooms, which are typically of lower biodiversity (Beans et al., 2008). The close similarity of diatom assemblages between the two interglacial facies, MIS 5e and Holocene, suggests that ocean temperature, circulation, and seasonal sea ice duration in the Adélie region were similar during these two interglacial periods (Fig. 5).

4.2.2 Glaciation MIS 5d–5a (interglacial to glacial transition)

The glaciation facies shows clear evidence for an increase in the influence of sea ice over the core site compared to the interglacial facies. The PC 2 assemblage starts to increase at this time, and the *Eucampia* index increases slightly (Fig. 5). *Fragilariopsis kerguelensis* reach maximum abundance early in the glaciation (Fig. 3), while the abundance of the *Fragilariopsis* group (dominated by *F. obliquecostata*) increases strongly throughout the glaciation, reaching a maximum abundance at the transition to MIS 4–2 (Fig. 3). Finally, the *Rhizosolenia* group, of which the cold-water species *Rhizosolenia antennata* var. *semispina* (Armand and Zielinski, 2011; Fig. 3) dominates, is found throughout the glaciation facies. Together, the PC 2 assemblage, *Fragilariopsis* species, *Eucampia* index and *Rhizosolenia ntennata* var. *semispina* suggest that the glaciation facies was characterised by an increase in the sea ice season relative to the MIS 5e interglacial.

The productivity proxies, Si/Al and biogenic silica are low, indicating a decrease in productivity throughout the glaciation (Fig. 5). However, the opposite is indicated by the continued presence of PC 1, which suggests high productivity.

The Shannon–Wiener index suggests that the late glaciation was a time of relatively high biodiversity (Fig. 5) relative to the MIS 5e and Holocene interglacials. This may be due to a more diversified environment, that is, the increased sea ice season and times of open water may have produced a more diversified community. In the modern-shelf environment, a greater diatom biodiversity is found near the Astrolabe Glacier rather than near the Mertz Glacier, where productivity is higher but fewer species dominate (Beans et al., 2008). Thus, the biodiversity in the samples may reflect this natural variability seen in the diatom assemblages in the Adélie region today.

4.2.3 Glacial (MIS 4–2)

Diatom assemblages can be used to subdivide the MIS 4–2 glacial interval into the early and late glacial stages (Fig. 5). The early glacial stage, comprising increased loadings of PC 1 (open ocean assemblage) and increasing loadings of PC 2 (sea ice assemblage), is similar to the glaciation, suggesting an initially prolonged sea ice season relative to the interglacial periods. The *Fragilariopsis* group is at its maximum in the early glacial (Fig. 3). After this initial increase

in PC 2, the assemblages align with high PC 1 only, suggesting temporary reversal of cooling and an increase in productivity. Overall glacial productivity in this region was low, with low Si/Al and biogenic silica. This is consistent with data from the broader Antarctic margin data (Bonn et al., 1998) and with the glaciation and deglacial facies. In the late glacial, from 160–100 cm, the assemblage displays a gradual increase in PC 2, suggesting an increase in the duration of the sea ice season (Fig. 5). After this, from 100–70 cm, the assemblages align with high PC 2, the sea ice assemblage, suggesting that the maximum duration of the sea ice season occurred towards the end of the late glacial (MIS 2). The increase in sea ice is further supported by the increase in the *Eucampia* index (Fig. 5).

The similarities in diatom assemblages between glaciation and the early glacial suggest that cooling of the ocean started long before the onset of the glacial and then continued gradually until the maximum sea ice duration (and therefore, cooling) was reached at the end of the last glacial (Fig. 5). This is consistent with gradual cooling reaching a maximum at the end of MIS 2, as seen in Antarctic ice cores (Jouzel et al., 1993) and in sea surface temperatures from global sediment cores (Kohfeld and Chase 2017), including records based on diatom assemblages from the Southern Ocean north of 56° S (Crosta et al., 2004; Chadwick et al., 2022; Jones et al., 2022). The assemblage composition of the late glacial is suggestive of a long sea ice season duration, an environment which, at present, occurs in the Ross and Weddell seas (Truesdale and Kellogg, 1979; Zielinski and Gersonde, 1997). This suggests that the permanent and/or summer sea ice edge, during the late glacial, was closer to the core site than it is today, indicating that the core site was covered by near-permanent sea ice during the peak glacial. However, the persistent presence of the *Thalassiosira lentiginosa* and PC 1 provides evidence that open ocean conditions existed over the Tan_44 site during part of the year.

4.2.4 Deglacials (glacial to interglacial transitions): MIS 2 to Holocene and MIS 6 to MIS 5e

The deglacial facies (between MIS 6 to MIS 5e and MIS 2 to Holocene) is generally associated with an increase in PC 1 (open ocean assemblage) and a decrease in PC 2 (sea ice assemblage) relative to the glacial (Fig. 5). The dominance of PC 1 suggests that there was high productivity throughout the deglacial, although the productivity proxies, biogenic silica and Si/Al, are low. The minor influence of *Thalassiothrix antarctica* (at 40 cm; Fig. 5), relative to the glacial period, suggests an increase in CDW occurred after the decline of sea ice (at 60 cm, at the end of the last glacial; Fig. 5) and prior to ice sheet retreat (at 15 cm, during the Holocene; Fig. 5). A similar sequence is observed within the MIS 6 to MIS 5e deglacial, but it is less clear. Here (at 270 cm; Fig. 5), the broken valves are abundant, but relative abundance is 0 %. Tolotti et al. (2013) and Li et al. (2021) also suggest, based on the presence of diatom species, that increased CDW influx occurred during the last deglacial in the Ross Sea and offshore Enderby Land, respectively. Lastly, the start of the MIS 2 and 1 deglacial (and the end of MIS 6 and 5 deglacial) is marked by a decrease in the PC 2 assemblage (Fig. 5), which suggests that the sea ice season duration declined rapidly at the end of the last glacial. This is consistent with the rapid sea ice retreat for the last two deglacial transitions from the distal Southern Ocean (at 56° S) documented by Crosta et al. (2004) and Chadwick et al. (2022).

In conclusion, the duration of the sea ice season decreased relatively rapidly and prior to CDW increase, as evidenced by *Thalassiothrix antarctica* (Fig. 5); this, in turn, occurred before the onset of ice sheet retreat (as indicated by IRD; Fig. 5). However, a more detailed study of diatom assemblages is needed in order to determine the relative timing and a more detailed chronology of these deglacial changes.

4.2.5 Diatom-barren MIS 6 glacial and micropyrite in MIS 6 to MIS 5e deglacial

The 350–320 cm interval is considered to be diatom-barren (Table S4). This may be due to the original assemblage having been affected by dilution at the sea floor by turbidity currents (Kellogg and Truesdale, 1979; Schrader et al., 1993; Escutia et al., 2003) or by a permanent sea ice cover, which reduced productivity, allowing only reworked diatoms to be transported to the site by bottom currents (Table S4). The presence of micropyrite within the 320–300 cm section suggests low oxygen levels could have prevailed during the time, brought on by either fast sedimentation, such as turbidity currents (Presti et al., 2011), or by an extensive sea ice cover (Lucchi and Rebesco, 2007). Interestingly, pyrite is also found within the 80–60 cm section, which comprises an increase of the reworked assemblage (PC 3; Fig. 5) at the end of the MIS 4–2 glacial facies.

5 Conclusion

Diatom assemblages in Tan_44 (64.5° S) varied on a glacial to interglacial timescale over the last 140 kyr, and their composition reflects in situ productivity but is also influenced slightly by bottom current reworking processes. The diatom assemblages were predominantly influenced by changes in sea ice duration and changing ocean circulation over the core site. The following is a summary of conclusions reached in this study (Fig. 6):

- The PC 1 assemblage dominance in the interglacial facies suggests that open ocean and seasonal sea ice environments during the MIS 5e and Holocene were similar to those of the present day. The close correspondence of assemblages between the two interglacials suggests that both surface water conditions related to sea surface

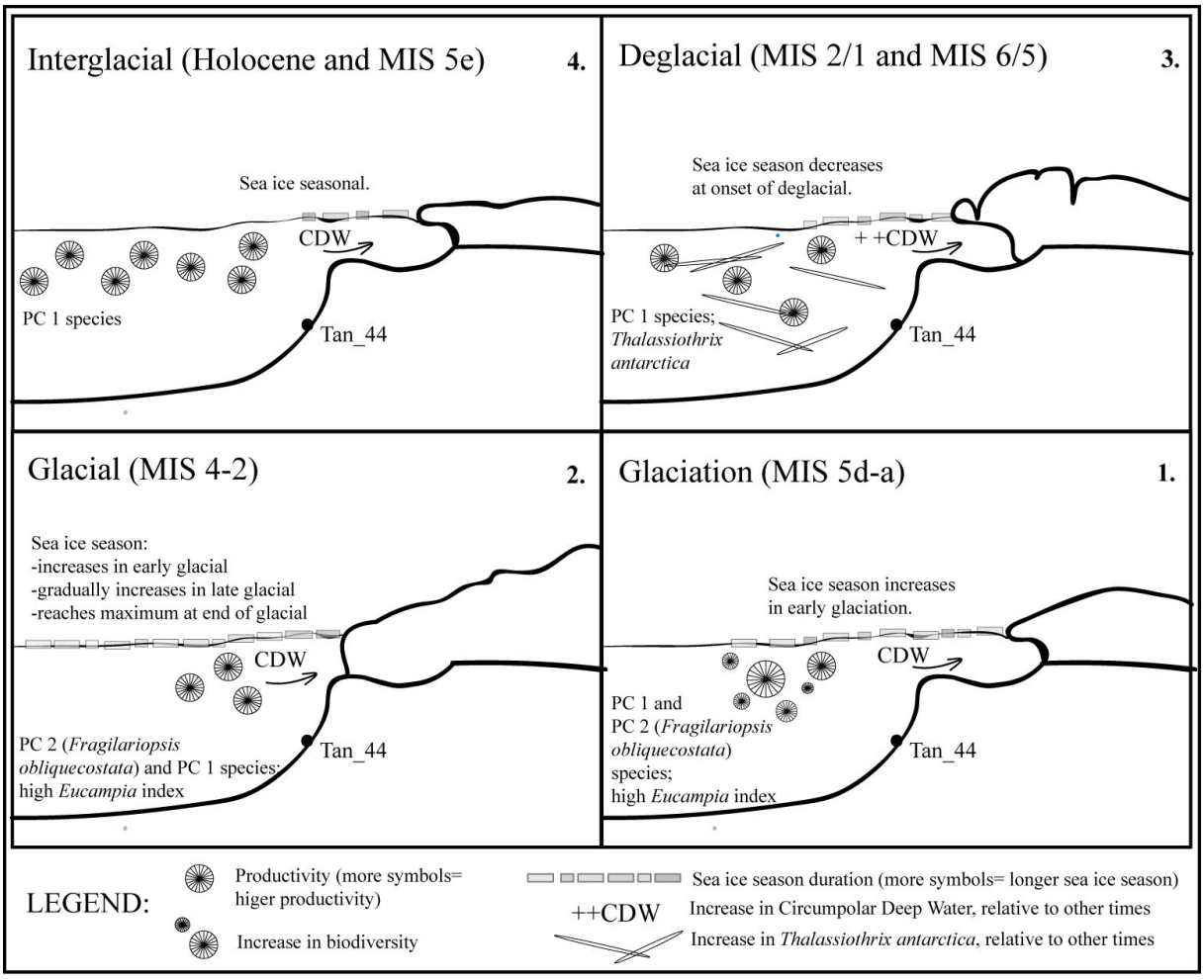

Figure 6. Sea ice and productivity interpretation across the last glacial cycle (∼ 140–∼ 5 ka) based on diatom assemblage variability. During the Holocene and MIS 5e interglacial periods, the seasonal sea ice at the site was similar to that of the present day. Sea ice duration initially increases, then decreases in glaciation (MIS 5d–a); and this also occurs in the early MIS 4–2 glacial. The sea ice then gradually increases during late MIS 4–2 glacial, reaching a maximum seasonal duration towards the end of the last glacial. During the deglacials (i.e., last two glacial-to-interglacial transitions), the influx rate of CDW increased relative to modern influx rates or other times, as suggested by the presence of the high-nutrient species, *Thalassiothrix antarctica*. This study suggests the sea ice decreased at the end of the last glacial and that the increase in CDW influx occurred after the sea ice season declined, during the last deglacial. Yet, all of this occurred before the onset of the last major ice sheet retreat.

temperature and sea ice duration were similar between the two interglacials.

- The unusually high dominance of *Thalassiosira lentiginosa* in the PC 1 assemblage in the interglacial facies suggests the assemblage was slightly affected by dissolution and also by reworking by bottom currents.
- The duration of the sea ice season, as indicated by the presence of PC 2, started to increase during the early glaciation stage (MIS 5d–5a) and in the early MIS 4–2 glacial and continued to increase throughout the late MIS 4–2 glacial, reaching a maximum extent towards the end of the glacial (MIS 2).
- However, the presence of both PC 2 and PC 1 assemblages during the MIS 4–2 glacial provides evidence that the summer sea ice edge was located further south than the core site, at 64.5° S in the Adélie region.
- The rapid decrease of the PC 2 sea ice assemblage suggests that a decline in the sea ice season occurred at the end of the last glacial.
- *Thalassiothrix antarctica* was found to be abundant in both deglacials, suggesting an increase of high-nutrient water. This influx is interpreted here as an increase in upwelling of CDW in the Adélie region during these times.

- Based on the diatom assemblages and the IRD increase in the Tan_44 core, the sea ice retreated prior to the increase in CDW upwelling during the last deglacial, which was then followed by an increase in IRD, indicating the retreat of the ice sheet.
- Biodiversity was highest during the glaciation stage and the start of the last glacial and was lowest during the late glacial and the interglacial periods. The higher biodiversity during glaciation and the start of the glacial could be the result of a more diversified environment relative to other periods.

This new diatom data set provides an understanding of the changes in sea ice proximal to East Antarctica over the last glacial cycle. It provides new insight into the extent of the summer sea ice in the last glacial and the winter sea ice extent during the last interglacial and also suggests changes within seasonal sea ice with respect to the upwelling of CDW during climate (glacial-to-interglacial) transitions. These are important parameters to constrain climate models to understand the importance of the influence of Antarctic sea ice on global climate over the last 140 kyr. Further marine sediment core data (increased resolution and more cores) are required to improve our understanding of the spatial and temporal changes in sea ice proximal to Antarctica.

Data availability. The data are available at PANGAEA: https://doi.org/10.1594/PANGAEA.946549 (Pesjak et al., 2022).

Supplement. The supplement related to this article is available online at: https://doi.org/10.5194/cp-19-419-2023-supplement.

Author contributions. LP carried out diatom identification, counts and statistical analysis under the guidance of AM. The sedimentological analysis was performed by LP, under the guidance of HB, and the geochemical analysis was performed by LP under the guidance of ZC. The age model was determined by LP, under the guidance of ZC and HB. LP has prepared the manuscript, with contributions from all authors.

Competing interests. The contact author has declared that none of the authors has any competing interests.

Disclaimer. Publisher's note: Copernicus Publications remains neutral with regard to jurisdictional claims in published maps and institutional affiliations.

Special issue statement. This article is part of the special issue "Reconstructing Southern Ocean sea-ice dynamics on glacial-to-historical timescales". It is not associated with a conference.

Acknowledgements. We acknowledge the National Institute of Water and Atmospheric Research (NIWA), Wellington, New Zealand, and the crew and scientists from R/V *Tangaroa* 2013 voyage lead by Mike Williams. This TAN1302 voyage was funded by New Zealand, Australian, and French research agencies. The core was originally logged on board the ship by Molly Patterson. Taryn Noble assisted with u-channel preparation at NIWA in Wellington, while the XRF scanning was completed by Patricia Gadd at ANSTO laboratories in Sydney. We further acknowledge Nils Jansen, who assisted with biogenic silica analyses at IMAS; Lisa Northcote, who assisted in grain size analysis; and Geraldine Jacobs and Alan William at the Australian Nuclear Science and Technology (ANSTO), who coordinated ^{14}C analysis. We also acknowledge the funding for ^{14}C dating, provided by ANSTO Research Portal Proposal 10705.

Financial support. This research was supported under the Australian Research Council's Special Research Initiative for the Antarctic Gateway Partnership (project no. SR140300001).

Review statement. This paper was edited by Xavier Crosta and reviewed by Matthew Chadwick and one anonymous referee.

References

Alley, R. B., Anandakrishnan, S., Christianson, K., Horgan, H. J., Muto, A., Parizek, B. R., Pollard, D., and Walker, R. T.: Oceanic forcing of ice-sheet retreat: West Antarctica and more, Annu. Rev. Earth Planet. Sci., 43, 207–231, 2015.

Armand, L. K. and Zielinski, U., Diatom species of the genus Rhizosolenia from Southern Ocean sediments: distribution and taxonomic notes, Diatom Res., 16, 259–294, 2011.

Armand, L. K., Crosta, X., Romero, O., and Pichon, J. J.: The biogeography of major diatom taxa in Southern Ocean sediments: 1. Sea ice related species, Palaeogeogr. Palaeocl. Palaeoecol., 223, 93–126, 2005.

Arndt, J. E., Schenke, H. W., Jakobsson, M., Nitsche, F. O., Buys, G., Goleby, B., Rebesco, M., Bohoyo, F., Hong, J., Black, J., and Greku, R.: 'The International Bathymetric Chart of the Southern Ocean (IBCSO) Version 1.0 – A new bathymetric compilation covering circum-Antarctic waters, Geophys. Res. Lett., 40, 3111–3117, 2013.

Arrigo, K. R. and Van Dijken, G. L.: Phytoplankton dynamics within 37 Antarctic coastal polynya systems, J. Geophys. Res.-Oceans, 108, 3271, https://doi.org/10.1029/2002JC001739, 2003.

Beans, C., Hecq, J. H., Koubbi, P., Vallet, C., Wright, S., and Goffart, A.: A study of the diatom-dominated microplankton summer assemblages in coastal waters from Terre Adélie to the Mertz Glacier, East Antarctica (139° E–145° E), Polar Biol., 31, 1101–1117, 2008.

Bonn, W. J., Gingele, F. X., Grobe, H., Mackensen, A., and Fütterer, D. K.: Palaeoproductivity at the Antarctic continental margin: opal and barium records for the last 400 ka, Palaeogeogr. Palaeocl. Palaeoecol., 139, 195–211, 1998.

Burckle, L. H.: Ecology and palaeoecology of the marine diatom Eucampia antarctica (Castr.) Mangin, Mar. Micropaleontol., 9, 77–86, 1984.

Caburlotto, A., De Santis, L., Zanolla, C., Camerlenghi, A., and Dix, J.: New insights into Quaternary glacial dynamic changes on the George V Land continental margin (East Antarctica), Quaternary Sci. Rev., 25, 3029–3049, 2006.

Caburlotto, A., Lucchi, R. G., De Santis, L., Macri, P., and Tolotti, R.: Sedimentary processes on the Wilkes Land continental rise reflect changes in glacial dynamic and bottom water flow, Int. J. Earth Sci., 99, 909–926, 2010.

Chadwick, M., Crosta, X., Esper, O., Thöle, L., and Kohfeld, K. E.: Compilation of Southern Ocean sea-ice records covering the last glacial-interglacial cycle (12–130 ka), Clim. Past, 18, 1815–1829, https://doi.org/10.5194/cp-18-1815-2022, 2022.

Cody, R. D., Levy, R. H., Harwood, D. M., and Sadler, P. M.: Thinking outside the zone: High-resolution quantitative diatom biochronology for the Antarctic Neogene. Palaeogeogr. Palaeocl. Palaeoecol., 260, 92–121, 2008.

Cook, C. P., van de Flierdt, T., Williams, T., Hemming, S. R., Iwai, M., Kobayashi, M., Jimenez-Espejo, F. J., Escutia, C., González, J. J., Khim, B. K., McKay, R. M., Passchier, S., Bohaty, S. M., Riesselman, C. R., Tauxe, L., Sugisaki, S., Galindo, A. L., Patterson, M. O., Sangiorgi, F., Pierce, E. L., Brinkhuis, H., Klaus, A., Fehr, A., Bendle, J. A. P., Bijl, P. K., Carr, S. A., Dunbar, R. B., Flores, J. A., Hayden, T. G., Katsuki, K., Kong, G. S., Nakai, M., Olney, M. P., Pekar, S. F., Pross, J., Röhl, U., Sakai, T., Shrivastava, P. K., Stickley, C. E., Tuo, S., Welsh, K., and Yamane, M.: Dynamic behaviour of the East Antarctic ice sheet during Pliocene warmth, Nat. Geosci., 6, 1017–1025, 2013.

Cooke, D. W. and Hayes, J. D.: Estimates of Antarctic Ocean seasonal sea-ice cover during glacial intervals, Antarct. Geosci., 131, 1017–1025, 1982.

Crosta, X., Strum, A., Armand, L. K., and Pichon, J. J.: Late Quaternary sea ice history in the Indian sector of the Southern Ocean as recorded by diatom assemblages, Mar. Micropaleontol., 50, 209–223, 2004.

Crosta, X., Romero, O., Armand, L. K., and Pichon, J. J.: The biogeography of major diatom taxa in Southern Ocean sediments: 2. Open ocean related species, Palaeogeogr. Palaeocl. Palaeoecol., 223, 66–92, 2005.

Crosta, X., Debret, M., Denis, D., Courty, M. A., and Ther, O.: Holocene long- and short-term climate changes off Adélie Land, East Antarctica, Geochem. Geophy. Geosy., 8, Q11009, https://doi.org/10.1029/2007GC001718, 2007.

Crosta, X., Kohfeld, K. E., Bostock, H. C., Chadwick, M., Du Vivier, A., Esper, O., Etourneau, J., Jones, J., Leventer, A., Müller, J., Rhodes, R. H., Allen, C. S., Ghadi, P., Lamping, N., Lange, C., Lawler, K.-A., Lund, D., Marzocchi, A., Meissner, K. J., Menviel, L., Nair, A., Patterson, M., Pike, J., Prebble, J. G., Riesselman, C., Sadatzki, H., Sime, L. C., Shukla, S. K., Thöle, L., Vorrath, M.-E., Xiao, W., and Yang, J.: Antarctic sea ice over the past 130,000 years, Part 1: A review of what proxy records tell us, EGUsphere [preprint], https://doi.org/10.5194/egusphere-2022-99, 2022.

DeMaster, D. J.: The supply and accumulation of silica in the marine environment, Geochim. Cosmochim. Ac., 45, 1715–1732, 1981.

Depoorter, M. A., Bamber, J., Griggs, J., Lenaerts, J. T., Ligtenberg, S. R., van den Broeke, M. R., and Moholdt, G.: Calving fluxes and basal melt rates of Antarctic ice shelves, Nature, 502, 89–92, 2013.

Diekmann, B., Fütterer, D., Grobe, H., Hillenbrand, C., Kuhn, G., Michels, K., Petschick, R., and Pirrung, M.: Terrigenous sediment supply in the polar to temperate South Atlantic: Land-ocean links of environmental changes during the late Quaternary, in: The South Atlantic in the Late Quaternary: Reconstruction of material budgets and current systems, edited by: Wefer, G., Mulitza, S., and Ratmeyer, V., Springer-Verlag, Berlin, Heidelberg, Germany, 375–399, ISBN 3540210288, 2004.

Domack, E., Jull, A. T., Anderson, J., Linick, T., and Williams, C.: Application of tandem accelerator mass-spectrometer dating to late Pleistocene-Holocene sediments of the East Antarctic continental shelf, Quatern. Res., 31, 277–287, 1989.

Domack, E. W.: Sedimentology of glacial and glacial marine deposits on the George V-Adelie continental shelf, East Antarctica, Boreas, 11, 79–97, 1982.

Escutia, C., Warnke, D., Acton, G. D., Barcena, A., Burckle, L., Canals, M., and Frazee, C. S.: Sediment distribution and sedimentary processes across the Antarctic Wilkes Land margin during the Quaternary, Deep-Sea Res. Pt. II, 50, 1481–1508, 2003.

Fetterer, F., Knowles, K., Meier, W. N., Savoie, M., and Windnagel, A. K.: 2017 updated daily, Sea Ice Index', Version 3, NSIDC – National Snow and Ice Data Center, Boulder, Colorado, USA, https://doi.org/10.7265/N5K072F8, 2017.

Fink, D., Hotchkis, M., Hua, Q., Jacobsen, G., Smith, A. M., Zoppi, U., Child, D., Mifsud, C., van der Gaast, H., and Williams, A.: The antares AMS facility at ANSTO, Nucl. Instrum. Meth. Phys. Res. B, 223, 109–115, 2004.

Fryxell, G.: Comparison of winter and summer growth stages of the diatom Eucampia antarctica from the Kerguelen Plateau and south of the Antarctic convergence zone, Proc. ODP. Sci. Results, 119, 675–685, 1991.

Gadd, P. S. and Heijnis, H. H.: The potential of ITRAX core scanning: applications in quaternary science, Paper presented at the AQUA Biennial Meeting, 29 June–4 July 2014, The Grand Hotel, Mildura, https://apo.ansto.gov.au/dspace/handle/10238/9381 (last access: 8 February 2023), 2014.

Garrison, D. L. and Buck, K. R.: The biota of Antarctic pack ice in the Weddell Sea and Antarctic Peninsula regions, Polar Biol., 10, 211–219, 1989.

Gersonde, R. and Zielinski, U.: The reconstruction of late Quaternary Antarctic sea-ice distribution- the use of diatoms as a proxy for sea-ice, Palaeogeogr. Palaeocl. Palaeoecol., 162, 263–286, 2000.

Gersonde, R., Crosta, X., Abelmann, A., and Armand, L.: Sea-surface temperature and sea ice distribution of the Southern Ocean at the EPILOG Last Glacial Maximum-a circum-Antarctic view based on siliceous microfossil records, Quaternary Sci. Rev., 24, 869–896, 2005.

Grobe, H. and Mackensen, A.: Late Quaternary climatic cycles as recorded in sediments from the Antarctic continental margin, in: The Antarctic paleoenvironment: A perspective on Global Change, Antarctic Research Series 56, American Geophysical Union, 349–376, https://doi.org/10.1016/j.quascirev.2021.107069, 1992.

Hartman, J. D., Sangiorgi, F., Barcena, M. A., Tateo, F., Giglio, F., Albertazzi, S., Trincardi, F., Bijl, P. K., Langone, L., and Asioli, A.: Sea-ice, primary productivity and ocean temperatures at the Antarctic marginal zone during late Pleistocene, Quaternary Sci. Rev., 266, 497–506, https://doi.org/10.1017/S0954102007000697, 2021.

Helm, V., Humbert, A., and Miller, H.: Elevation and elevation change of Greenland and Antarctica derived from CryoSat-2, The Cryosphere, 8, 1539–1559, https://doi.org/10.5194/tc-8-1539-2014, 2014.

Holder, L., Duffy, M., Opdyke, B., Leventer, A., Post, A., O'Brien, P., and Armand, L. K.: Controls since the mid-Pleistocene transition on sedimentation and primary productivity downslope of Totten Glacier, East Antarctica, Paleoceanogr. Paleocl., 35, e2020PA003981, https://doi.org/10.1029/2020PA003981, 2020.

Hua, Q., Jacobsen, G. E., Zoppi, U., Lawson, E. M., Williams, A. A., Smith, A. M., and McGann, M. J.: Progress in radiocarbon target preparation at the ANTARES AMS Centre, Radiocarbon, 43, 275–282, 2001.

IBN: IBN SPSS Statistics documentation, https://www.ibm.com/docs/en/spss-statistics, last access: 20 July 2020.

Jacobs, S. S.: On the nature and significance of the Antarctic Slope Front, Mar. Chem., 35, 9–24, 1991.

Johansen, J. R. and Fryxell, G. A.: The genus Thalassiosira (Bacillariophyceae): studies on species occurring south of the Antarctic Convergence Zone, Phycologia, 24, 155–179, 1985.

Jones, J., Kohfeld, K. E., Bostock, H., Crosta, X., Liston, M., Dunbar, G., Chase, Z., Leventer, A., Anderson, H., and Jacobsen, G.: Sea ice changes in the southwest Pacific sector of the Southern Ocean during the last 140 000 years, Clim. Past, 18, 465–483, https://doi.org/10.5194/cp-18-465-2022, 2022.

Jouzel, J., Barkov, N., Barnola, J., Bender, M., Chappellaz, J., Genthon, C., Kotlyakov, V., Lipenkov, V., Lorius, C., and Petit, J.: Extending the Vostok ice-core record of paleoclimate to the penultimate glacial period, Nature, 364, 407–412, 1993.

Kaczmarska, I., Barbrick, N., Ehrman, J., and Cant, G.: Eucampia Index as an indicator of the Late Pleistocene oscillations of the winter sea-ice extent at the ODP Leg 119 Site 745B at the Kerguelen Plateau, in: Twelfth International Diatom Symposium, 30 August–5 September 1992, Renesse, the Netherlands, 103–112, 1993.

Kellogg, T. B. and Truesdale, R. S.: Late Quaternary paleoecology and paleoclimatology of the Ross Sea: the diatom record, Mar. Micropaleontol., 4, 137–158, 1979.

Knox, G. A.: Biology of the Southern Ocean, in: 2nd Edn., Marine Biology Series, edited by: Lutz, P. L., CRC Press, Taylor and Francis Group, University of Canterbury, Christchurch, New Zealand, 531 pp., ISBN 0849333946, 2006.

Kohfeld, K. E. and Chase, Z.: Temporal evolution of mechanisms controlling ocean carbon uptake during the last glacial cycle, Earth Planet. Sc. Lett., 472, 206–215, 2017.

Kopczyńska, E. E., Weber, L., and El-Sayed, S.: Phytoplankton species composition and abundance in the Indian sector of the Antarctic Ocean, Polar Biol., 6, 161–169, 1986.

Kopczyńska, E. E., Fiala, M., and Jeandel, C.: Annual and interannual variability in phytoplankton at a permanent station off Kerguelen Islands, Southern Ocean, Polar Biol., 20, 342–351, 1998.

Leventer, A.: Modern distribution of diatoms in sediments from the George V Coast, Antarctica, Mar. Micropaleontol., 19, 315–332, 1992.

Leventer, A., Domack, E., Dunbar, R., Pike, J., Stickley, C., Maddison, E., Brachfeld, S., Manley, P., and McClennen, C.: Marine sediment record from the East Antarctic margin reveals dynamics of ice sheet recession, GSA Today, 16, 4, https://doi.org/10.1130/GSAT01612A.1, 2006.

Li, Q., Xiao, W., Wang, R., and Chen, Z.: Diatom based reconstruction of climate evolution through the Last Glacial Maximum to Holocene in the Cosmonaut Sea, East Antarctica, Deep-Sea Res. Pt II, 194, 104960, https://doi.org/10.1016/j.dsr2.2021.104960, 2021.

Ligowski, R.: Phytoplankton of the Olaf Prydz Bay (Indian Ocean, East Antarctica) in February 1969, Polish Polar Res., 4, 21–32, 1983.

Ligowski, R., Godlewski, M., and Lukowski, A.: Sea ice diatoms and ice edge planktonic diatoms at the northern limit of the Weddell Sea pack ice, in: Proceedings of the NIPR Symposium on Polar Biology, 5, March 1992, Japan, 9–20, 1992.

Lisiecki, L. E. and Raymo, M. E.: A Pliocene-Pleistocene stack of 57 globally distributed benthic δ^{18}O records, Paleoceanography, 20, PA1003, https://doi.org/10.1029/2004PA001071, 2005.

Lucchi, R. G. and Rebesco, M.: Glacial contourites on the Antarctic Peninsula margin: insight for palaeoenvironmental and palaeoclimatic conditions, Geol. Soc. Lond. Spec. Publ., 276, 111–127, 2007.

Lucchi, R. G., Rebesco, M., Camerlenghi, A., Busetti, M., Tomadin, L., Villa, G., Persico, D., Morigi, C., Bonci, M. C., and Giorgetti, G.: Mid-late Pleistocene glacimarine sedimentary processes of a high-latitude, deep-sea sediment drift (Antarctic Peninsula Pacific margin), Mar. Geol., 189, 343–370, 2002.

Maddison, E. J., Pike, J., and Dunbar, R.: Seasonally laminated diatom-rich sediments from Dumont d'Urville Trough, East Antarctic margin: Late-Holocene neoglacial sea-ice conditions, Holocene, 22, 857–875, 2012.

Massom, R. A., Scambos, T. A., Bennetts, L. G., Reid, P., Squire, V. A., and Stammerjohn, S. E.: Antarctic ice shelf disintegration triggered by sea ice loss and ocean swell, Nature, 558, 383–389, 2018.

Masson-Delmotte, V., Schulz, M., Abe-Ouchi, A., Beer, J., Ganopolski, A., González Rouco, J. F., Jansen, E., Lambeck, K., Luterbacher, J., Naish, T., Osborn, T., Otto-Bliesner, B., Quinn, T., Ramesh, R., Rojas, M., Sha,o X., and Timmermann A.: Information from Paleoclimate Archives, in: Climate change 2013: the physical science basis, Cambridge University Press, 383–464, https://doi.org/10.1017/CB9781107415324.013, 2013.

McMinn, A.: Late Holocene increase in sea ice extent in fjords of the Vestfold Hills, eastern Antarctica, Antarct. Sci., 12, 80–88, 2000.

McMinn, A., Heijnisj, H., Harle, K., and McOrist, G.: Late-Holocene climatic change recorded in sediment cores from Ellis Fjord, eastern Antarctica, Holocene, 11, 291–300, 2001.

Medlin, L. K. and Priddle, J. (Eds.): Polar marine diatoms, the British Antarctic Survey, Natural Environmental Research Council, High Cross, Madingley Road, Cambridge, UK, 214 pp., ISBN 0856651400, 1990.

Mezgec, K., Stenni, B., Crosta, X., Masson-Delmotte, V., Baroni, C., Braida, M., Ciardini, V., Colizza, E., Melis, R., Salvatore, M.

C., and Severi, M.: Holocene sea ice variability driven by wind and polynya efficiency in the Ross Sea, Nat. Commun., 8, 1–12, 2017.

Minowa, M., Sugiyama, S., Ito, M., Yamane, S., and Aoki, S.: Thermohaline structure and circulation beneath the Langhovde Glacier ice shelf in East Antarctica, Nat. Commun., 12, 1–9, 2021.

Moisan, T. and Fryxell, G.: The distribution of Antarctic diatoms in the Weddell Sea during austral winter, Botanica Marina, 36, 489–498, 1993.

Mortlock, R. A. and Froelich, P .N.: A simple method for the rapid determination of biogenic opal in pelagic marine sediments, Deep-Sea Res. Pt. A, 36, 1415–1426, 1989.

Orsi, A. H., Whitworth III, T., and Nowlin Jr., W. D.: On the meridional extent and fronts of the Antarctic Circumpolar Current, Deep-Sea Res. Pt. I, 42, 641–673, 1995.

Passchier, S.: Linkages between East Antarctic Ice Sheet extent and Southern Ocean temperatures based on a Pliocene high-resolution record of ice-rafted debris off Prydz Bay, East Antarctica, Paleoceanography, 26, PA4204, https://doi.org/10.1029/2010PA002061, 2011.

Patterson, M. O., McKay, R., Naish, T., Escutia, C., Jimenez-Espejo, F. J., Raymo, M. E., Meyers, S. R., Tauxe, L., Brinkhuis, H., Klaus, A., Fehr, A., Bendle, J. A. P., Bijl, P. K., Bohaty, S. M., Carr, S. A., Dunbar, R. B., Flores, J. A., Gonzalez, J. J., Hayden, T. G., Iwai, M., Katsuki, K., Kong, G. S., Nakai, M., Olney, M. P., Passchier, S., Pekar, S. F., Pross, J., Riesselman, C. R., Röhl, U., Sakai, T., Shrivastava, P. K., Stickley, C. E., Sugasaki, S., Tuo, S., van de Flierdt, T., Welsh, K., Williams, T., and Yamane, M.: Orbital forcing of the East Antarctic ice sheet during the Pliocene and Early Pleistocene, Nat. Geosci., 7, 841–847, 2014.

Peck, V. L., Allen, C. S., Kender, S., McClymont, E. L., and Hodgson, D. A.: Oceanographic variability on the West Antarctic Peninsula during the Holocene and the influence of upper circumpolar deep water, Quaternary Sci. Rev., 119, 54–65, 2015.

Pesjak, L.: The variability of ocean circulation, productivity, and sea ice in the Adélie region, East Antarctica, over the last two glacial cycles, PhD thesis, University of Tasmania, https://doi.org/10.25959/100.00047523, 2022.

Pesjak, L., McMinn, A., Chase, Z., and Bostock, H.: Relative abundance of diatom species, biogenic silica and Si/Al over last ∼ 140 kyr, from the East Antarctic continental margin, PANGAEA [data set], https://doi.org/10.1594/PANGAEA.946549, 2022.

Pichon, J. J., Bareille, G., Labracherie, M., Labeyrie, L. D., Baudrimont, A., and Turon, J. L.: Quantification of the biogenic silica dissolution in Southern Ocean sediments, Quatern. Res., 37, 361–378, 1992.

Post, A., Galton-Fenzi, B., Riddle, M., Herraiz-Borreguero, L., O'Brien, P., Hemer, M., McMinn, A., Rasch, D., and Craven, M.: Modern sedimentation, circulation and life beneath the Amery Ice Shelf, East Antarctica, Cont. Shelf Res., 74, 77–87, 2014.

Presti, M., Barbara, L., Denis, D., Schmidt, S., De Santis, L., and Crosta, X.: Sediment delivery and depositional patterns off Adélie Land (East Antarctica) in relation to late Quaternary climatic cycles, Mar. Geol., 284, 96–113, 2011.

Pritchard, H., Ligtenberg, S. R., Fricker, H. A., Vaughan, D. G., van den Broeke, M. R., and Padman, L.: Antarctic ice-sheet loss driven by basal melting of ice shelves, Nature, 484, 502–505, 2012.

Pritchard, H. D., Arthern, R. J., Vaughan, D. G., and Edwards, L. A.: Extensive dynamic thinning on the margins of the Greenland and Antarctic ice sheets, Nature, 461, 971–975, 2009.

Pudsey, C. J.: Late Quaternary changes in Antarctic Bottom Water velocity inferred from sediment grain size in the northern Weddell Sea, Mar. Geol., 107, 9–33, 1992.

Pudsey, C. J. and Camerlenghi, A.: 'Glacial–interglacial deposition on a sediment drift on the Pacific margin of the Antarctic Peninsula, Antarct. Sci., 10, 286–308, 1998.

Quilty, P. G., Kerry, K. R., and Marchant, H. J.: A seasonally recurrent patch of Antarctic planktonic diatoms, Search (Sydney), 16, 1–2, 1985.

Reimer, P.J., Bard, E., Bayliss, A., Beck, J. W., Blackwell, P. G., Ramsey, C. B., Buck, C. E., Cheng, H., Edwards, R. L., Friedrich, M., and Grootes, P. M.: IntCal13 and Marine13 radiocarbon age calibration curves 0–50,000 years cal BP, Radiocarbon, 55, 1869–1887, 2013.

Rembauville, M., Blain, S., Armand, L., Quéguiner, B., and Salter, I.: Export fluxes in a naturally iron-fertilized area of the Southern Ocean – Part 2: Importance of diatom resting spores and faecal pellets for export, Biogeosciences, 12, 3171–3195, https://doi.org/10.5194/bg-12-3171-2015, 2015.

Rignot, E., Mouginot, J., Scheuchl, B., Van Den Broeke, M., Van Wessem, M. J., and Morlighem, M.: Four decades of Antarctic Ice Sheet mass balance from 1979–2017, P. Natl. Acad. Sci. USA, 116, 1095–1103, 2019.

Romero, O. E., Armand, L. K., Crosta, X., and Pichon, J. J.: The biogeography of major diatom taxa in Southern Ocean surface sediments: 3. Tropical/Subtropical species, Palaeogeogr., Palaeocl. Palaeoecol., 223, 49–65, 2005.

Rothwell, R. G. and Croudace, I. W. (Eds.): Twenty Years of XRF Core Scanning Marine Sediments: What Do Geochemical Proxies Tell Us?, in: Micro-XRF Studies of Sediment Cores, Springer, Dordrecht, the Netherlands, 25–102, https://doi.org/10.1007/978-94-017-9849-5_2, 2015.

Salabarnada, A., Escutia, C., Röhl, U., Nelson, C. H., McKay, R., Jiménez-Espejo, F. J., Bijl, P. K., Hartman, J. D., Strother, S. L., Salzmann, U., Evangelinos, D., López-Quirós, A., Flores, J. A., Sangiorgi, F., Ikehara, M., and Brinkhuis, H.: Paleoceanography and ice sheet variability offshore Wilkes Land, Antarctica – Part 1: Insights from late Oligocene astronomically paced contourite sedimentation, Clim. Past, 14, 991–1014, https://doi.org/10.5194/cp-14-991-2018, 2018.

Schrader, H., Swanberg, I. L., Burckle, L. H, and Grønlien, L.: Diatoms in recent Atlantic (20° S to 70° N latitude) sediments: abundance patterns and what they mean, in: Twelwth International Diatom Symposium, 30 August–5 September 1992, Renesse, the Netherlands, 129–135, 1993.

Scott, F. J. and Thomas, D. P.: Diatoms, Antarctic marine protists, edited by: Scott, F. J. and Marchant, H. J., Australian Biological Resources Study/ Australian Antarctic Division, Canberra, Australia, 13–201, 2005.

Shemesh, A., Burckle, L., and Froelich, P.: Dissolution and preservation of Antarctic diatoms and the effect on sediment thanatocoenoses, Quatern. Res., 31, 288–308, 1989.

Shi, G. R.: Multivariate data analysis in palaeoecology and palaeobiogeography – a review, Palaeogeogr. Palaeocl. Palaeoecol. 105, 199–234, 1993.

Silvano, A., Rintoul, S. R., Peña-Molino, B., Hobbs, W. R., van Wijk, E., Aoki, S., Tamura, T., and Williams, G. D.: Freshening by glacial meltwater enhances melting of ice shelves and reduces formation of Antarctic Bottom Water, Sci. Adv., 4, eaap9467, https://doi.org/10.1126/sciadv.aap9467, 2018.

Smith, J. A., Hillenbrand, C. D., Pudsey, C. J., Allen, C. S., and Graham, A. G.: The presence of polynyas in the Weddell Sea during the Last Glacial Period with implications for the reconstruction of sea-ice limits and ice sheet history, Earth Planet. Sc. Lett., 296, 287–298, 2010.

Spellerberg, I. F. and Fedor, P. J.: A tribute to Claude Shannon (1916–2001) and a plea for more rigorous use of species richness, species diversity and the 'Shannon–Wiener' Index, Global Ecol. Biogeogr., 12, 177–179, 2003.

Spreen, G., Kaleschke, L., and Heygster, G.: Sea ice remote sensing using AMSR-E 89-GHz channels, J. Geophys. Res.-Oceans, 113, C02S03, https://doi.org/10.1029/2005JC003384, 2008.

Stuiver, M. and Polach, H. A.: Discussion reporting of ^{14}C data, Radiocarbon, 19, 355–363, 1977.

Taylor, F. and McMinn, A.: Evidence from diatoms for Holocene climate fluctuation along the East Antarctic margin, Holocene, 11, 455–466, 2001.

Taylor, F., McMinn, A., and Franklin, D.: Distribution of diatoms in surface sediments of Prydz Bay, Antarctica, Mar. Micropaleontol., 32, 209–229, 1997.

Tolotti, R., Salvi, C., Salvi, G., and Bonci, M.C., Late Quaternary climate variability as recorded by micropaleontological diatom data and geochemical data in the western Ross Sea, Antarctica, Antarct. Sci., 25, 804–820, 2013.

Tooze, S., Halpin, J. A., Noble, T. L., Chase, Z., O'Brien, P. E., and Armand, L.: Scratching the surface: A marine sediment provenance record from the continental slope of central Wilkes Land, East Antarctica, Geochem. Geophy. Geosy., 21, e2020GC009156, https://doi.org/10.1029/2020GC009156, 2020.

Torricella, F., Melis, R., Malinverno, E., Fontolan, G., Bussi, M., Capotondi, L., Del Carlo, P., Di Roberto, A., Geniram, A., Kuhn, G., and Khim, B. K.: Environmental and Oceanographic Conditions at the Continental Margin of the Central Basin, Northwestern Ross Sea (Antarctica) Since the Last Glacial Maximum, Geosciences, 11, 155, https://doi.org/10.3390/geosciences11040155, 2021.

Truesdale, R. S. and Kellogg, T. B.: Ross Sea diatoms: modern assemblage distributions and their relationship to ecologic, oceanographic, and sedimentary conditions, Marine Micropaleontology, 4, 13-31, 1979.

Warnock, J. P. and Scherer, R. P.: Diatom species abundance and morphologically-based dissolution proxies in coastal Southern Ocean assemblages, Cont. Shelf Res., 102, 1–8, 2015.

Williams, G., Bindoff, N., Marsland, S., and Rintoul, S.: Formation and export of dense shelf water from the Adélie Depression, East Antarctica, J. Geophys. Res.-Oceans, 113, C04039, https://doi.org/10.1029/2007JC004346, 2008.

Williams, G., Aoki, S., Jacobs, S., Rintoul, S., Tamura, T., and Bindoff, N.: Antarctic bottom water from the Adélie and George V Land coast, East Antarctica (140–149° E), J. Geophys. Res.-Oceans, 115, C04027, https://doi.org/10.1029/2009JC005812, 2010.

Williams, G., Herraiz-Borreguero, L., Roquet, F., Tamura, T., Ohshima, K., Fukamachi, Y., Fraser, A., Gao, L., Chen, H., and McMahon, C. The suppression of Antarctic bottom water formation by melting ice shelves in Prydz Bay, Nat. Commun., 7, 12577, https://doi.org/10.1038/ncomms12577, 2016.

Williams, M.: RV Tangaroa Voyage Report Tan1302 – Mertz Polynya Voyage 1 February to 14 March 2013, NIWA, Wellington, New Zealand, 19–33, 2013.

Wilson, D. J., Bertram, R. A., Needham, E. F., van de Flierdt, T., Welsh, K. J., McKay, R. M., Mazumder, A., Riesselman, C. R., Jimenez-Espejo, F. J., and Escutia, C.: Ice loss from the East Antarctic Ice Sheet during late Pleistocene interglacials, Nature, 561, 383–386, https://doi.org/10.1038/s41586-018-0501-8, 2018.

Wu, L., Wang, R., Xiao, W., Ge, S., Chen, Z., and Krijgsman, W.: Productivity-climate coupling recorded in Pleistocene sediments off Prydz Bay (East Antarctica), Palaeogeogr. Palaeocl. Palaeoecol., 485, 260–270, 2017.

Zielinski, U. and Gersonde, R.: Diatom distribution in Southern Ocean surface sediments (Atlantic sector): Implications for paleoenvironmental reconstructions, Palaeogeogr. Palaeocl. Palaeoecol., 129, 213–250, 1997.

Zielinski, U. and Gersonde, R.: Plio–Pleistocene diatom biostratigraphy from ODP Leg 177, Atlantic sector of the Southern Ocean, Mar. Micropaleontol., 45, 225–268, 2002.